Chapter 2

Ocean Thermal Energy Conversion: Technological Readiness and Indonesia Progress

Ristiyanto Adiputra, Rasgianti, Erwandi, Ariyana Dwiputra Nugraha, Navik Puryantini, & Takeshi Yasunaga

A. Ocean for Clean Energy Development

Global energy consumption has increased over the last three decades (IEA, 2020) followed by an increase in non-renewable energy production from fossil fuels (IEA, 2021). Continuation of these conditions triggers climate change and global warming, directly affecting human health (Naing et al., 2019), human prosperousness (Calleja-Agius et al., 2021) and environmental sustainability (Shukla et al., 2017). Therefore, the need and the urgency for clean energy is undeniable.

Global renewable energy potential is estimated to reach 5,016.3 TWh (Moriarty & Wang, 2015) where ocean energy sources have a promising potential of about 10 TW (Esteban & Leary, 2012). One of the ocean energy resources with a promising, underutilized energy

R. Adiputra, Rasgianti, Erwandi, A. D. Nugraha, N. Puryantini, & T. Yasunaga
National Research and Innovation Agency, e-mail: ristiyanto.adiputra@brin.go.id

Adiputra, R., Rasgianti, Erwandi, Nugraha, A. D. Puryantini, N. & Yasunaga, T. (2023). Ocean thermal energy conversion: Technological readiness and Indonesia progress. In A. Kiswantono & R. M. Shoedarto (Eds.), *Indonesia's Energy Transition Preparedness Framework Towards 2045* (23–86). BRIN Publishing. DOI: 10.55981/brin.892.c812
E-ISBN: 978-623-8372-41-6

source is Ocean Thermal Energy Conversion (OTEC). It uses the temperature difference between warm surface and cold deep seawater to generate energy (Nihous & Vega, 1993). OTEC is advantageous because it produces no greenhouse gas emissions during operation, can run without fuel, and provides many ancillary benefits besides energy. The energy produced by OTEC has the potential to replace fossil fuels (Wang et al., 2011). Despite its many advantages, OTEC has yet to be widely deployed, remains largely unexplored and untapped at its potential sites.

Analysis of OTEC technology and development problems is compiled comprehensively by reviewing the global current state of OTEC technology and system optimization. The review covers various aspects, starting with a detailed examination of the technical aspects of OTEC, including the advances made in supporting components, support structures, working systems within the OTEC domain, OTEC side benefits, and OTEC environmental impacts. In addition, the assessment of the economic implications associated with using and developing OTEC would be discussed. The economic analysis includes critical factors such as levelized cost of energy (LCOE) and initial capital calculations. By examining these economic aspects, this chapter aims to shed light on OTEC projects' financial viability and potential return on investment in Indonesia.

B. Ocean Thermal Energy Conversion System

OTEC power plants generate electrical energy by taking advantage of the temperature difference between warm seawater at the surface and cold seawater at depth. Roughly speaking, the amount of energy produced by OTEC power plants is equal to the amount of thermal energy extracted from the seawater. The OTEC system was first proposed by D'Arsonval in 1881, who introduced the use of marine thermal energy by using cyclic heat engines to generate electricity (Kobayashi et al., 2001). The basic principle of the OTEC system is to use the surface heat of seawater to evaporate the working fluid. The vapor produced is then directed to drive the turbine and then converted

into electrical energy by the generator. The vapor coming out of the turbine is then returned to liquid by utilizing the cold temperature of deep ocean water. Based on the type of cycle, OTEC systems can be divided into three main categories, namely closed-cycle, open-cycle, and hybrid cycle.

1. Closed-cycle OTEC

Closed-cycle OTEC uses cyclic heat engines with working fluid that are placed in a closed cycle where there is no direct contact between the seawater and the working fluid. The Rankine cycle is one example of simple closed cycles, but is widely used in closed thermodynamic cycles. The Rankine cycle system consists of an evaporator, condenser, water pump, turbine and generator, and working fluid pump (see Figure 2.1). The Rankine cycle has four thermal processes, namely isentropic compression, isentropic heating, isentropic expansion, and isobaric condensation (Yang & Yeh, 2014). In the Rankine cycle, fluids with low boiling points require smaller turbines for higher efficiency (Ganic & Moeller, 1980).

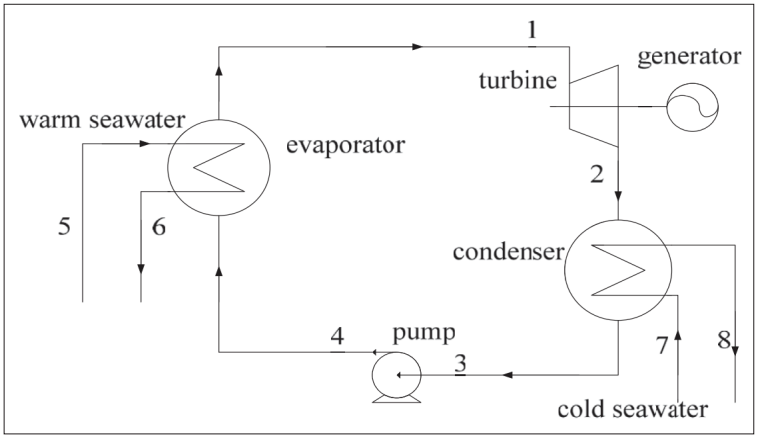

Source: Chen et al. (2019)

Figure 2.1 Closed-cycle OTEC System Flow Diagram

In the closed-cycle OTEC, heat transfer occurs in the evaporator. The heat transfer from the warm seawater brings the working fluid to saturated vapor state. The vapor then passes through the turbine to the lower pressure zone and moves it. The movement of the turbine is then converted into electrical energy by the generator. The saturated vapor is then returned to liquid form in the condenser using the low temperature of cold seawater. The success of the Rankine cycle depends on how much energy is recovered from the cycle. As the vapor expands through the turbine, it gets energy, then used some of the energy to return to its liquid state. Due to isothermal evaporation and condensation of the working fluid, irreversible losses in the heat exchange process are inevitable for the Rankine cycle. As a result, it limits the improvement of the system performance. When the temperature difference between warm seawater and cold seawater is about 15–25°C, the maximum thermal efficiency of the Rankine cycle is about 3% (Nakaoka & Uehara, 1988).

Closed-cycle OTEC calculation is similar to the Rankine cycle, in which the calculation is based on a T-S diagram as shown in Figure 2.2. The thermal efficiency of closed-cycle OTEC is significantly affected by the power generated in the turbine ($W_T W_T$) and the power required to drive the working fluid pump ($W_p W_p$). The calculation of the thermal efficiency of the cycle has been formulated as Equation (2.1) (Chen et al., 2019).

$$\eta = \frac{W_{net}}{Q_E} = \frac{W_T - W_P}{Q_E} = \frac{(h_1 - h_2) - (h_4 - h_3)}{h_1 - h_4} \qquad (2.1)$$

Where:

W_{net} : Net output power of system

Q_E : Total heat of warm surface seawater

: $M_f(h_1 - h_2)$

W_p : Power of the working fluid pump

: $M_f(h_4 - h_3)$

W_T : Work in the turbine
: $M_f(h_2 - h_3)$
M_f : Mass flow rate of the working fluid
h : Specific enthalpy.

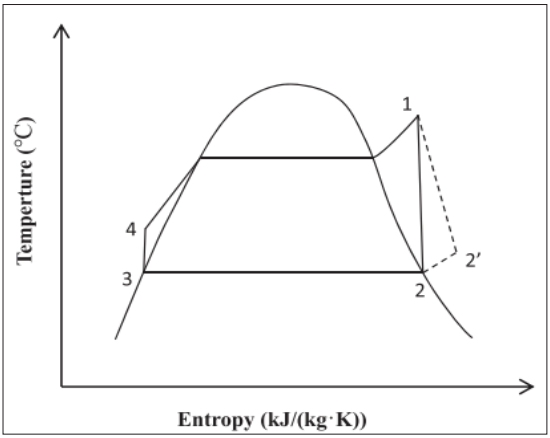

Source: Chen et al. (2019)

Figure 2.2 T-S Diagram of the Rankine Cycle

Several studies have been carried out to improve the efficiency of closed-cycle OTEC systems as reviewed in Liu et al. (2020). Aydin et al. (2014) investigated the use of solar energy to improve cycle efficiency. The study was conducted by comparing two closed cycle systems. In the first system, solar energy was used to raise the temperature of the warm seawater before it entered the evaporator (Figure 2.3). Meanwhile, in the second system, solar energy is used to heat the working fluid to a superheated state before it passes through the turbine. Aydin et al. (2014) concluded that under the same conditions, the thermal efficiency of the first and second cycle was 1.9% and 3%, respectively.

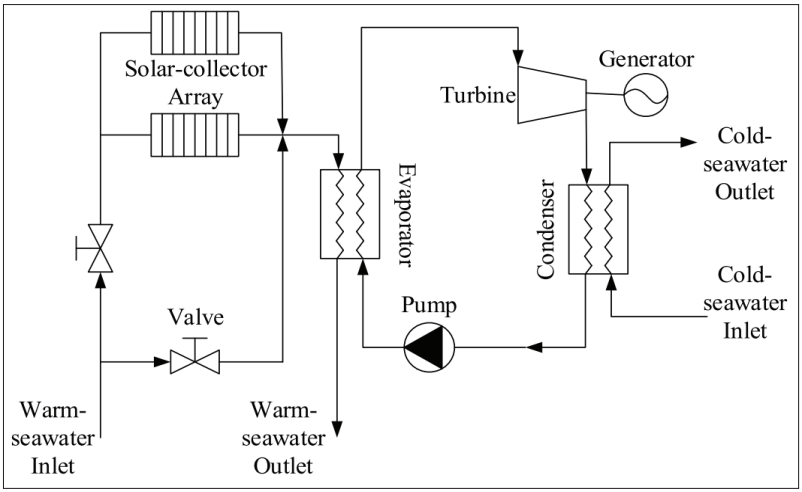

Source: Liu et al. (2020)

Figure 2.3 Solar-boosted OTEC Diagram

On the other hand, Lee et al. (2015) use ejectors to optimize turbine work output and improve cycle thermal efficiency in closed-cycle OTEC as shown in Figure 2.4. Vapor ejectors are used to ensure the pressure difference between the turbine outlet and the condensing pressure of the working fluid. This results in an increase in turbine 2 work output for a given volume of circulating working fluid. The conclusion is that the change in nozzle diameter of the ejector has the greatest effect on the thermal efficiency of the cycle. Even so, a larger diameter does not necessarily result in a higher level of efficiency, but rather needs to be in an optimal setting. At the most optimal setting, the thermal efficiency of the system reaches 2.47%, while the efficiency of the Rankine cycle under the same conditions is only 2.2%.

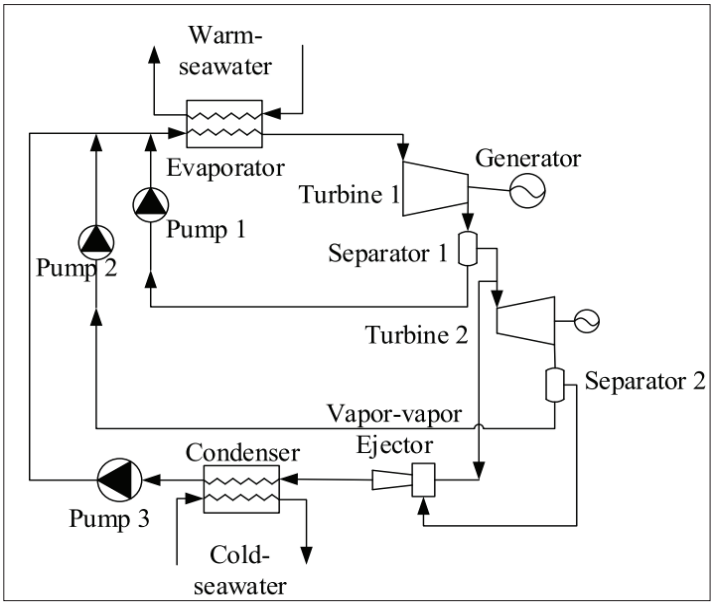

Source: Liu et al. (2020)

Figure 2.4 Vapor Ejector OTEC Diagram

2. Open-Cycle OTEC

Open-cycle OTEC was first proposed by G. Claude in the late 1920s to address the high cost and biofouling potential of closed-cycle OTEC. The diagram of the open-cycle OTEC can be seen in Figure 2.5. The main difference between open-cycle and closed-cycle OTEC is the use of warm seawater as the working fluid. The warm seawater is evaporated by lowering its boiling point by adjusting the vacuum pressure on the evaporator. As in the closed cycle, the vapor is then used to drive turbines (Masutani & Takahashi, 2001). In general, open-cycle OTECs have lower efficiencies than closed-cycle OTECs and require anti-corrosive materials for the production facility due to the salinity of the working fluid. However, open-cycle OTECs can produce desalinated water as a byproduct, which is 0.5–0.6% of the warm seawater input used by the cycle (Mutair & Ikegami, 2014).

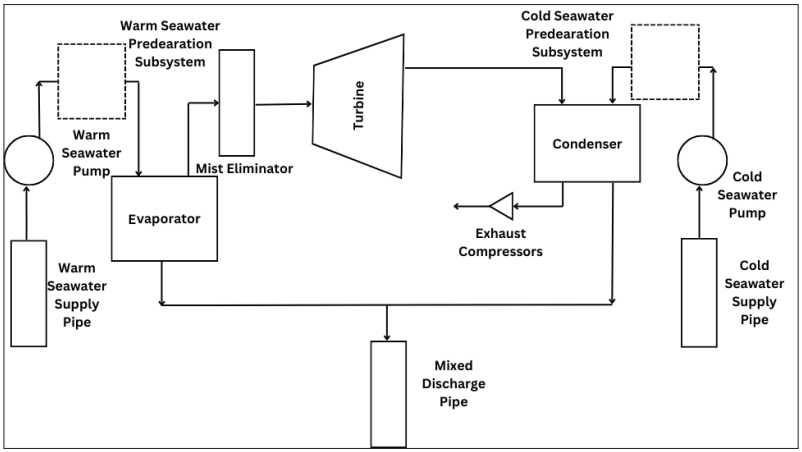

Source: Elaborated based on Link & Parsons (1986)

Figure 2.5 Open-cycle OTEC System Flow Diagram

Unlike closed-cycle OTEC, the entire open-cycle OTEC system operates under partial vacuum conditions (Bharathan et al., 1990). Open-cycle OTEC uses seawater as the working fluid, in which seawater is evaporated by lowering the boiling point of seawater by reducing the pressure below saturation pressure in the evaporator. The vapor produced in the evaporator is a relatively pure vapor. The transfer of heat energy occurs from most of the warm seawater to a small portion of the mass of warm seawater that becomes vapor (Masutani & Takahashi, 2001). Less than about 0.5–0.6% of the liquid warm seawater entering the flash evaporator is converted to vapor. As in other cycles, the vapor then passes through the turbine at low pressure, which then converts its motion into electrical energy by the generator (Bharathan et al., 1990).

As shown in Figure 2.6, the open cycle production of net electricity and desalinated water can be flexible with the use of multiple condensers as designed by Kim et al. (2016). The warm seawater vapor produced by the evaporator is divided into turbines for power generation and E-condensers for primary desalination. The vapor

from the turbine then flows to the T- and D-condensers for secondary desalination and disposal. Uncondensed vapor is removed from the system by a vacuum compressor. Based on testing in four modes (power generation only, desalination only, half desalination and half power without recycling, and half desalination and half power with recycling), Kim et al. (2016) concluded that the half desalination and half power mode produces 50% less electrical energy than the power generation mode alone. For the seawater desalination results in a 206 kW generator, both the half-desalination and half-power modes and the desalination mode produce 3.5 kg/s of fresh water per 113.05 kg/s of seawater.

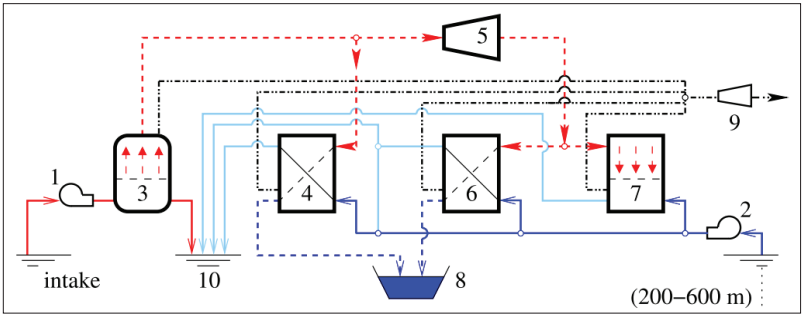

Note: Numbers indicate as follows: (1) pump for warm surface water, (2) pump for cold deep-sea water, (3) flash evaporator, (4) E-condenser, (5) a turbine, (6) T-condenser, (7) D-condenser, (8) fresh water reservoir, (9) vacuum compressor, and (10) open sea

Source: Kim et al. (2016)

Figure 2.6 Multiple Condenser Open-cycle OTEC

Hernández-Romero et al. (2022) optimized the performance of the open-cycle OTEC system by combining ocean thermal energy with solar thermal energy. The optimization is focused on cycle performance in generating electricity and desalinated water. Solar thermal energy is collected through solar collectors to then be used to increase the temperature of warm seawater before it reaches the evaporator. Optimization is carried out in two operational modes, namely by prioritizing electricity production and desalination water

production. In the mode with priority of electricity production, at optimal conditions, it can generate 82,848 kW/year of electrical energy and 1366 m^3/year of desalinated water. On the other hand, in the mode with the priority of desalinated water, at ideal conditions, it can produce 3,575 m^3/year of desalinated water and 31,738 kW/year of electrical energy.

3. Hybrid Cycle OTEC

Open-cycle OTEC requires a large turbine, which also has a large inertia, to produce desalinated water (Vega, 2013). The large inertia decreases the difference of pressure between inlet and outlet part of turbine and reduced the efficiency of the turbine. Closed-cycle OTEC, on the other hand, requires a smaller turbine because the boiling point of the working fluid is much lower than seawater, making the system more efficient. Hybrid-cycle OTEC is designed to combine the previous two types of cycles to produce working fluid vapor, which is then used as desalinated water (Herrera et al., 2021).

In the OTEC hybrid cycle shown in Figure 2.7, warm seawater is evaporated in a partial vacuum. Warm seawater vapor then enters the heat exchanger to evaporate the working fluid (Panchal & Bell, 1987). Some of the warm seawater vapor condenses into desalinated water, while the working fluid vapor circulates through turbines and condenses in condensers. The working fluid vapor is then condensed on the condenser by transferring heat to the cold seawater. The non-condensable vapor is then compressed by a vacuum pump and vented to the atmosphere. The main weakness of the hybrid cycle is that there is a critical relationship between desalinated water production and power generation, so if one system experiences a problem, both systems cannot function (Masutani & Takahashi, 2001).

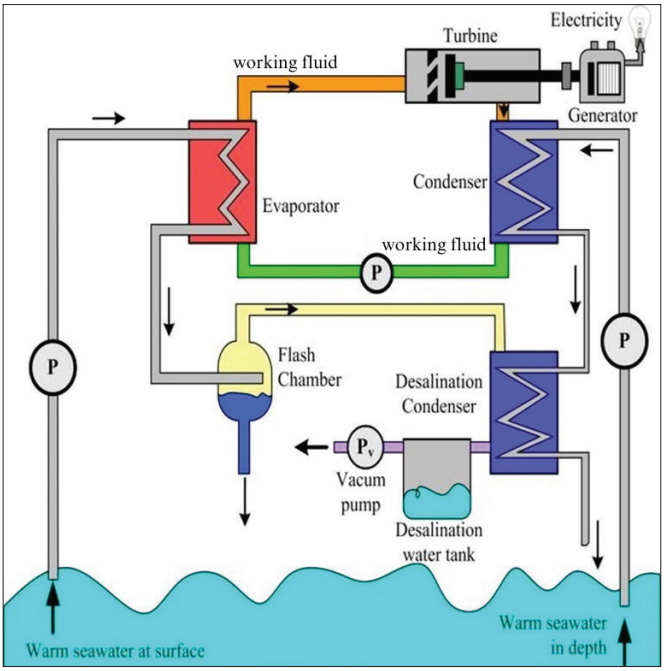

Source: Suparta (2020)

Figure 2.7 Hybrid-cycle OTEC System Flow Diagram

Uehara et al., (1996) compared the performance of power production as well as water production in a hybrid cycle with a closed-cyle combined with flash desalination process, which called integrated-hybrid cycle (Figure 2.8). Based on the optimization of existing design results, the net power output and desalinated water production of the integrated hybrid cycle is higher than that of the regular hybrid cycle (Panchal & Bell, 1987), while the overall cost performance may be required including maintenance and operation.

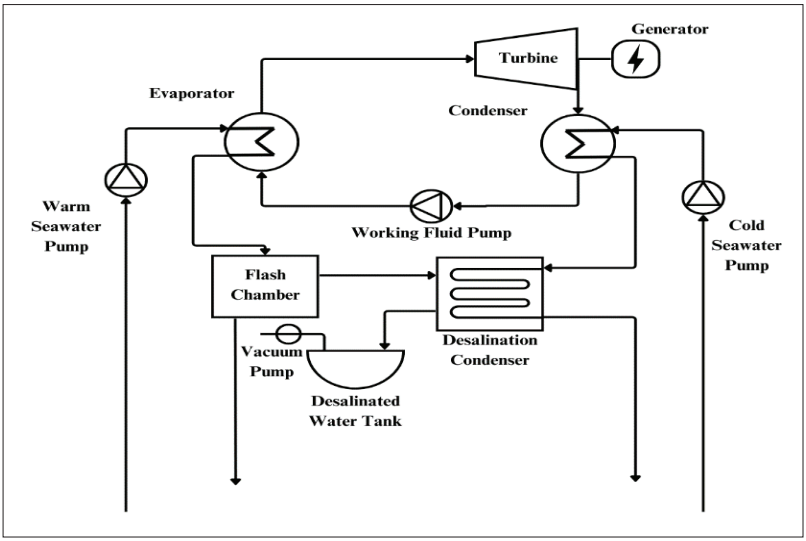

Source: Uehara et al. (1996)

Figure 2.8 Integrated-hybrid OTEC system combining a closed-cyle with flash desalination process

4. Working Fluid

In addition to the characteristics of the system, the working fluid has a significant impact on the efficiency of the OTEC cycle. Working fluids used in the OTEC cycle must have appropriate thermophysical properties and be stable over a specified temperature range. Working fluid selection must be based on thermal efficiency and cycle exergy, considering the economic value of the system (Liu et al., 2020). The working fluid commonly used in OTEC power plants is ammonia because its physical properties are ideal for the OTEC cycle (Wang et al., 2011). In his research on the Rankine cycle, Sun et al. (2012) concluded that ammonia is more ideal than refrigerant R134a which is made of ethane-based molecule as a working fluid in terms of net power output produced.

Samsuri et al. (2016) compared the efficiency of two types of working fluids for the Rankine OTEC cycle system. The two types of

working fluids are pure chemicals and pseudo-pure fluids. The working fluids used in the category of pure chemicals are ammonia, R134a, R143a, propane, and R22. As for the category of pseudo-pure fluids, they consist of ammonia-water mixtures, R410a, R470c, R404a, and R507a. The results, as shown in Figure 2.9, ammonia and ammonia-water mixtures have higher net power and efficiency than the other working fluids. However, a separator is required to ensure that water vapor from the liquid does not damage the turbine blade, especially in the case of ammonia-water mixtures. It has been demonstrated that an ammonia-water combination produces more net power and has a lower cost of the main product than pure ammonia. Although it requires additional separators and reduces cost efficiency, ammonia or an ammonia-water mixture is still the best working fluid to increase net power.

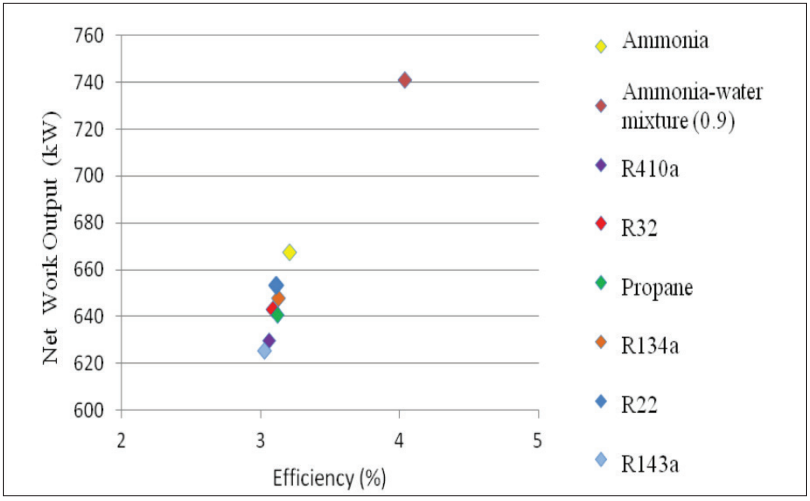

Source: Samsuri et al. (2016)

Figure 2.9 The Relationship between the Net Power Output and Efficiency

Figure 2.10 shows the Guo Hai cycle proposed by Liu et al. (2011). The Guo Hai cycle uses a mixture of ammonia and water as the working fluid. As in the Rankine cycle, the ammonia-water mixture is heated in an evaporator, but the ammonia vapor is then separated in a separator. A portion of the vapor is used to drive the turbine and then used to heat the working fluid in regenerator 2 until the working fluid reaches a saturated vapor state. The other portion of the ammonia vapor is then used to heat the working fluid in regenerator 1. The separation of the ammonia vapor allows the turbine to produce more net power. The heating of the working fluid in the Guo Hai cycle is more efficient than the regular Rankine cycle by combining the ammonia solution regenerative cycle and the extraction regenerative cycle in the system. The Guo Hai cycle can achieve a thermal efficiency of up to 5.16%.

The Kalina cycle, shown in Figure 2.11, uses a mixture of ammonia and water as the working fluid to vary the evaporation temperature (Kalina, 1984; Liu et al., 2020). The concentration of ammonia in the mixture decreases during the evaporation, raising the boiling point of the solution. This makes the process in accordance with the heat transfer process. The irreversible losses during the heat transfer process are significantly reduced, thus increasing the thermal efficiency (Kalina, 1983; Liu et al., 2020).

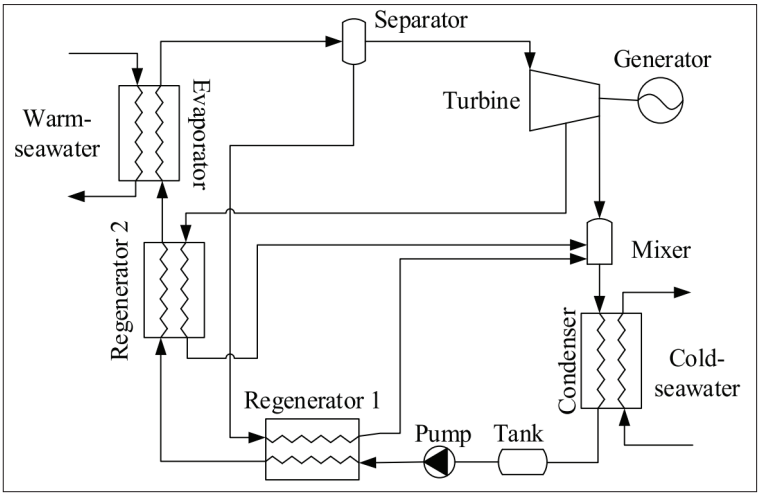

Source: Liu et al. (2011)

Figure 2.10 Guo Hai Cycle System Flow Diagram

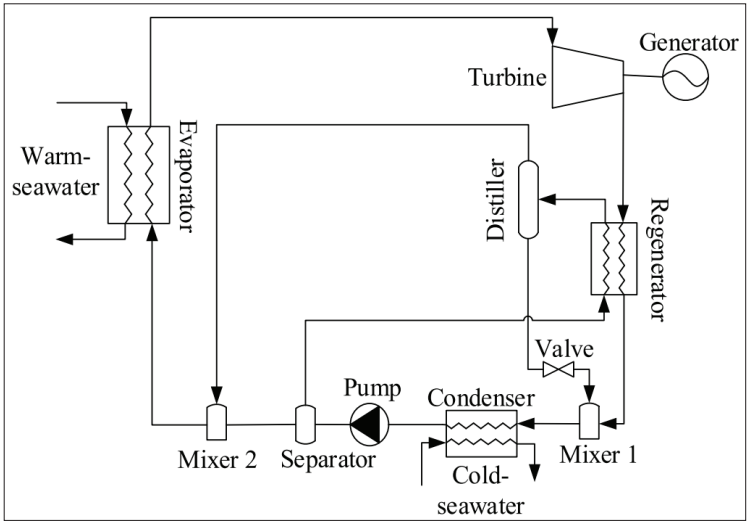

Source: Liu et al. (2020)

Figure 2.11 Kalina Cycle System Flow Diagram

The Uehara cycle, shown in Figure 2.12, uses an ammonia-water mixture as the working fluid and a two-stage turbine system (Uehara et al., 1998). In the Uehara cycle, the exhaust heat recovery stage is eliminated and replaced by ammonia heat recovery and a regenerative extraction cycle. The process is designed to minimize the irreversible loss of working fluid during the heat transfer process (Liu et al. 2011). Thus, the thermal efficiency of the Uehara cycle can reach 5.4%.

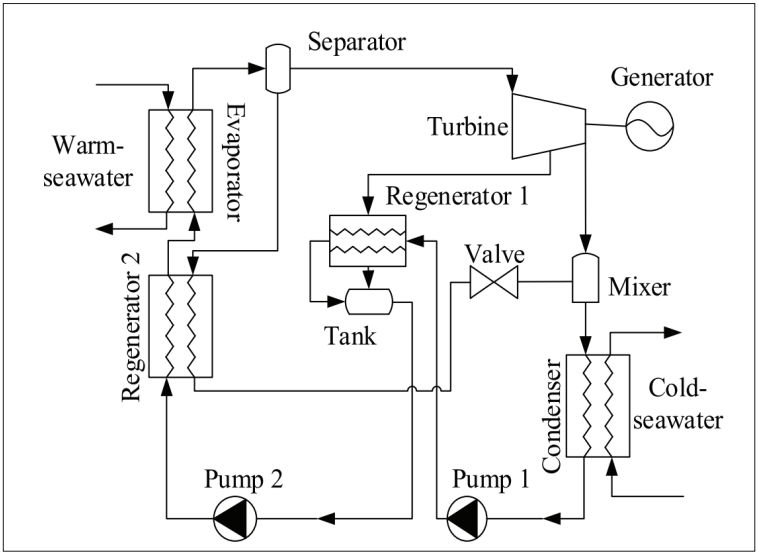

Source: Liu et al. (2020)

Figure 2.12 Uehara Cycle System Flow Diagram

5. Turbine

In the OTEC cycle, turbines are one of the main components in the process of producing electrical energy. Turbines are an important component in linking system displacement cycles and electrical energy output (Chen et al., 2022). Turbine outlet pressure is a key element in determining cycle efficiency (Wang et al., 2008). Closed-cycle OTEC typically uses a radial flow turbine as shown in Figure 2.13. The radial flow turbine has a high efficiency even though the power output and working fluid mass flow rate are minimal.

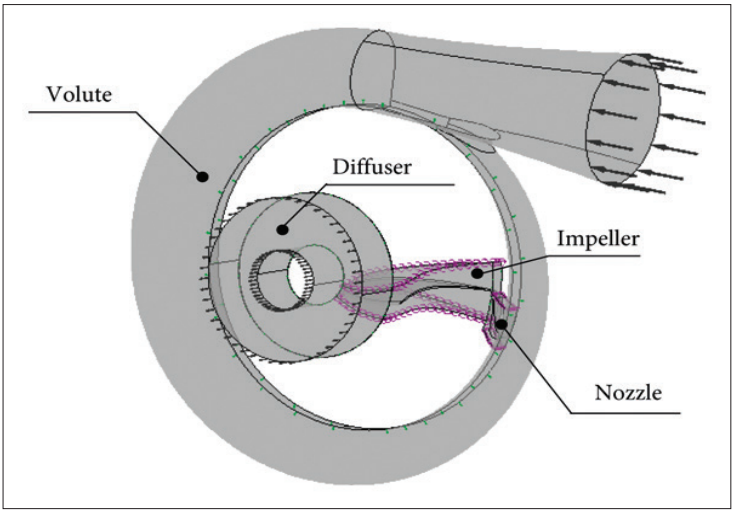

Source: Ma et al. (2022)

Figure 2.13 Radial Flow Turbine Model

Turbine efficiency is an important key to increasing net power output, especially due to the low overall cycle efficiency. Therefore, the aerodynamic design of the turbine must be carefully considered to maximize turbine efficiency. Some aerodynamic characteristics that have a major influence on turbine efficiency are impeller diameter ratio ($\overline{D}_2\overline{D}_2$), the degree of reaction ($\Omega\Omega$), and the velocity ratio ($\overline{u}_1$ $\overline{u}_1$) (Liu et al., 2020). The impeller diameter ratio is the ratio of the outlet diameter of the impeller to the inlet diameter of the impeller. The high and low impeller diameter ratio affects the operating capacity of the turbine. The degree of reaction is the ratio of the isentropic enthalpy droplets on the impeller to the decrease in total isentropic enthalpy. The degree of reaction represents the distribution of energy as the vapor expands in the nozzle and impeller. The velocity ratio is the ratio of the velocity of the vapor entering the impeller to the ideal velocity of the vapor under isentropic conditions. In addition to these three variables, there are four other variables that affect turbine

efficiency. Turbine efficiency is calculated using the formula shown in Equation (2.2) (Liu et al., 2020).

$$\eta = 2\bar{u}_1\left(\varphi\cos\alpha_1\sqrt{1-\Omega} - \bar{D}_2{}^2\bar{u}_1 + \bar{D}_2\psi\cos\beta_2\sqrt{\Omega + \psi^2(1-\Omega) + \bar{D}_2{}^2\bar{u}_1{}^2 - 2\bar{u}_1\varphi\cos\alpha_1\sqrt{1-\Omega}}\right) \quad (2.2)$$

Where :

$\bar{u}_1$ = Velocity ratio
$\bar{D}_2$ = Wheel diameter ratio
Ω = Degree of reaction
α_1 = Impeller inlet mounting angle
β_2 = Nozzle outlet mounting angle
φ = Coefficient of velocity of impeller
ψ = Coefficient of velocity of nozzle.

Chen et al. (2022) investigated the effect of nozzle blade installation angle and turbine internal flow field on turbine performance. According to the results of the analysis, the pressure and enthalpy increase as the nozzle blade installation angle increase. On the other hand, the power of the turbine shaft decreases with the increase of the nozzle blade installation angle. As the vapor velocity at the nozzle exit increases, the rotor will be damaged faster. However, if the vapor velocity at the nozzle exit is too low, the reverse flow and vortex flow will occur at the rotor inlet. Chen et al. (2022) concluded that 30.5° is the most optimal nozzle blade installation angle to optimize pressure fields and vapor speeds to maximize power output, efficiency, and durability.

The number of blades on the stator has a significant impact on turbine efficiency. The large number of stator blades makes the fluid flow more uniform, allowing the vapor to expand optimally in the stator. However, as more stator blades are added, friction loss rises

with the high contact between the vapor and the blades. Based on research by Chen et al. (2021), the total enthalpy loss of the turbine increases as the number of stator blades increases, while the reaction rate and enthalpy of the rotor decrease. In addition, the pressure at the stator outlet decreases as the number of stator blades increases, resulting in an increase in pressure drop. The increase and decrease in efficiency with the number of stator blades is shown in Figure 2.14, where it can be seen that the shaft output power increases as the number of stator blades increases, but the efficiency reaches its peak values at 27 blades.

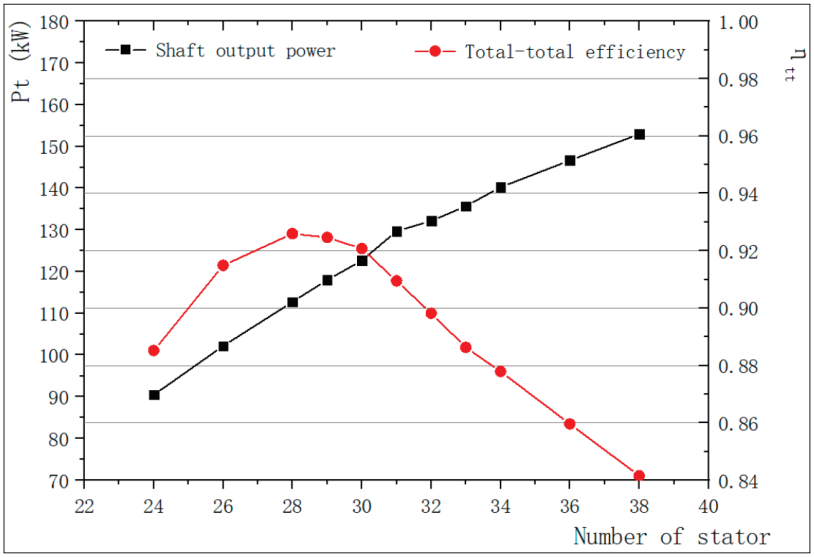

Source: Chen et al. (2021)

Figure 2.14 Effect of Number of Stator Blades on Turbine Shaft Power and Overall Efficiency

In addition to the number of blades, the shroud radius ratio and the hub radius ratio of the turbine stator also affect the turbine power output in the OTEC cycle. The shroud radius ratio has more influence on the turbine power output than the hub radius ratio (Alawadhi et al., 2020). As shown in Figure 2.15, for higher shroud radius ratio, the

turbine power output increases with increasing hub radius ratio, while for lower shroud radius ratio, the turbine power output decreases with increasing hub radius ratio.

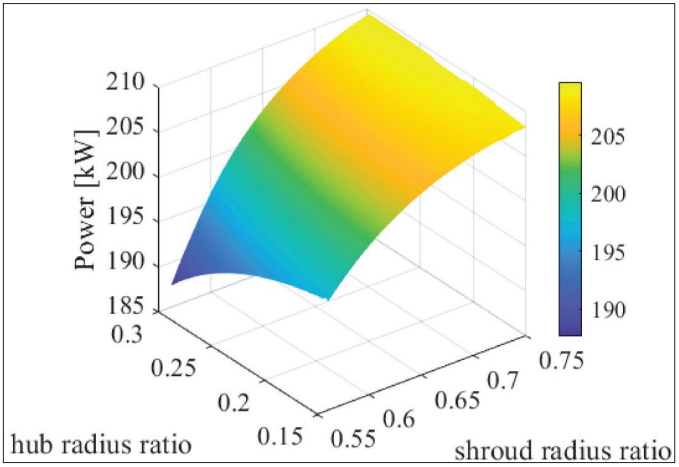

Source: Alawadhi et al. (2020)

Figure 2.15 Variation of the Power with Shroud Radius Ratio and Hub Radius Ratio

6. Available power of OTEC

In general, the calculation of the net power output and efficiency of the OTEC system is based on the amount of heat provided by the seawater in the system, as shown in Equation (2.1). On the other hand, Wu (1987) introduced a method to calculate the OTEC cycle efficiency in maximum power (η_{Pmax}) using surface seawater temperature (T_{ws}) and deep seawater temperature (T_{cs}) as shown in Equation (2.3). Wu's formula applies the finite time reversible heat engine proposed by Novikov (1958) as well as Curzon and Ahlborn (1975).

$$\eta_{Pmax} = 1 - \sqrt{\frac{T_{CS}}{T_{WS}}} \qquad (2.3)$$

Johnson (1983) proposes the exergy from seawater and compared the various cycles including closed and open cycles. The result shows the multistage open cycle will be the highest exergy efficiency. Yasunaga et al. (2021) shows the relationship between thermal efficiency and the work of heat engines in OTEC and propose to use the exergy efficiency for performance evaluation in OTEC by comparing the thermal efficiency and exergy efficiency in various designs of OTEC. Ikegami and Bejan (1998) theoretically expressed the relationship between the net power and thermal efficiency and exergy efficiency in OTEC. Yasunaga and Ikegami (2020) proposed the normalization of thermal efficiency to solve the discrepancy of the thermal efficiency and the work of heat engines. In short, the available power from the ideal heat engine W_m is expressed in Equation (2.4)

$$W_m = mc_p\left(\sqrt{T_{WS}} - \sqrt{T_{CS}}\right)^2 \tag{2.4}$$

where the mass flow rate and specific heat of surface and deep seawater is assumed same m (kg/s) and c_p (kJ/(kgK).

C. OTEC Supporting System

Almost all of the equipment at the land-based OTEC facility is installed onshore. This eliminates the need for electrical power transmission cables from power plants and mooring systems for cold water pipes (CWP) and floating platforms, as shown in Figure 2.16. Onshore plants also make it easier to distribute and use the desalinated water. However, the seawater pipe required in onshore plants is longer, requiring a pipe structure reinforcement system that can increase construction and maintenance costs.

The 10 MWe onshore OTEC model of the Panchal and Bell (1987) system can produce 2.25 million liters of desalinated water for every 1 MWe of electrical energy produced. This system is designed to increase desalinated water production by 60–80% by increasing heat transfer by 90% or by shutting down one of the turbines so that

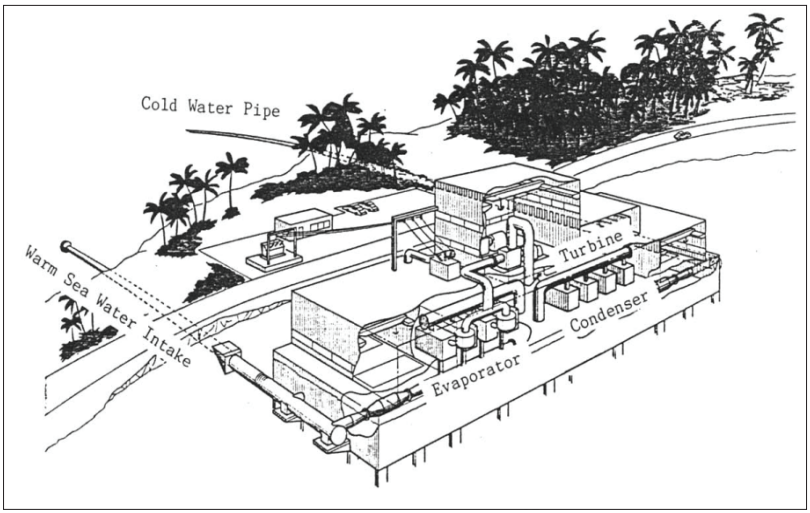

Source: Uehara et al. (1988)

Figure 2.16 Onshore OTEC Power Plant

ammonia vapor can flow directly into the condenser. However, in terms of electrical energy production, the cycle efficiency is only 1.6%.

All equipment in offshore facilities is located offshore or on floating platforms, unlike onshore facilities. With the use of floating platforms, CWPs are positioned vertically. As a result, their length and diameter are much smaller than those of onshore plants. However, due to the unstable nature of the ocean waves, floating platforms and CWPs' safety must be ensured during the operational life. To ensure that the floating platform and CWP are secure and will last throughout its operational life, a good mooring system design is required. Thus, OTEC floating platforms are often built on a large scale to increase structural stability, increase seakeeping, and minimize strain on the CWP (Wang et al., 2011).

As shown in Figure 2.17, Dr. Alfred Yee designed a floating platform to house the OTECs heat exchanger system and the turbine of the steel barge. In his design, the CWP is made of plastic and

is 825 meters long. It was designed to reach deep ocean water off the coast of the island of Hawaii. The plant became known as the Mini OTEC. It was capable of producing 50 kW gross power and 18 kW net power (Vega, 2002). The simple design of Mini OTEC then became a benchmark for several researchers to develop floating OTEC platforms.

1. Cold Water Pipe

One of the most important supporting components in OTEC plants, both onshore and offshore, is the cold-water pipe (CWP). CWP is used to supply water to the cooling system in the condenser. To obtain water at the correct temperature for condensing the working fluid vapor, a CWP of approximately 600–1,000 meters in length is required for both onshore and offshore plants. Power output affects the fluid flow required in the OTEC CWP (Nihous, 2007).

The first development of a CWP was made by Claude in 1933, Brazil. The CWP's diameter was 2.5 m and able to reach a depth of approximately 700 m in a vertical position (Avery & Wu, 1994). However, the CWP was destroyed in a storm, and the project was abandoned. Previously, Claude had also carried out experimental construction of a land-based facility in Cuba, but this also failed during the CWP installation phase. The failure occurred because the geography of the proposed site, which consists of a gentle underwater slope, would not allow the pipe to be laid all the way as planned. Problems with the CWP also led to the abandonment of the OTEC project in the port of Bengal, India (Avery & Wu, 1994; Miller & Ascari,, 2011).

The development of the OTEC CWP began after the 1973 oil crisis. The development also considered several important issues, such as material, connection system to the hull, and installation. As a result, pipes made of fiber reinforced polymer (FRP) using a sandwich-structured wall design were considered the most promising for installation and use, as shown in Figure 2.18. One of the successfully operating CWPs has a limited diameter of only 1–2 m and is used for a demonstration of power plants (Miller et al., 2012). CWPs

with the desired diameter to produce the right amount of energy are still very challenging to made in the overall OTEC system and components, compared to other components, such as the floating structure and deep water mooring (Hisamatsu & Utsunomiya, 2022).

The CWP must be both strong and lightweight to withstand continuous loads and movements, yet easy to install (Xiang et al., 2013). In the CWP design process, studies on strength analysis, pipe coupling movement analysis, and floating structure analysis, as well as the effect caused by internal flow analysis, are extremely important and are strongly considered. Adiputra and Utsunomiya (2019) state there are three main problems of OTEC CWP: analysis of strength either for general and in extreme collapse condition; analysis of CWP and vessel joint; and vibration occurs in the pipe, specifically vibration due to vortex and effect caused by internal flow.

Griffin (1981) proposed a tube design for a net power of 40 MW. Griffin proposed an OTEC with a diameter of 9.2 m and a length of 1,000 m, as shown in Figure 2.19. The CWP has a rigid wall with a flexible joint configuration with several supporting components in the CWP, such as hydraulic seal, center support, wall support, and pin connector. The design did not state the exact material properties but only mention the materials under consideration for CWP construction including steel, concrete, fiber reinforced plastic (FRP), thermoplastics and elastomers/fabrics. In this way, when released, the OTEC will be able to withstand the existing forces, such as the hydrodynamic force, as well as the forces generated by the floating platform (Griffin, 1981).

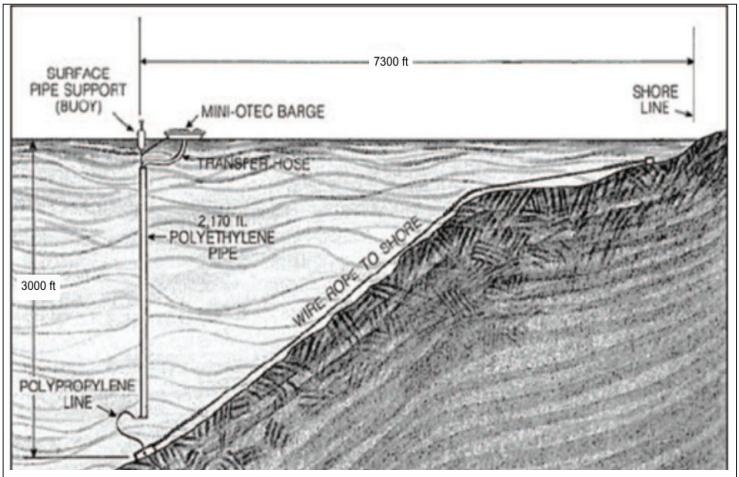

(a)

(b)

Note: (a) Cold water pipe model; (b) Floating platform

Source: Wang et al. (2011)

Figure 2.17 Offshore MINI OTEC Power Plant

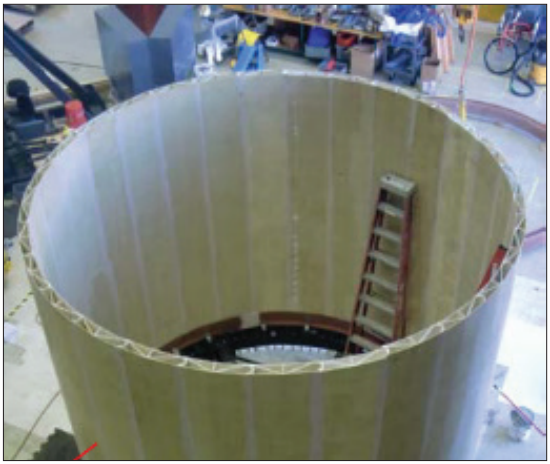

Source: Miller et al. (2012)

Figure 2.18 OTEC CWP with FRP and Sandwich Structure Design

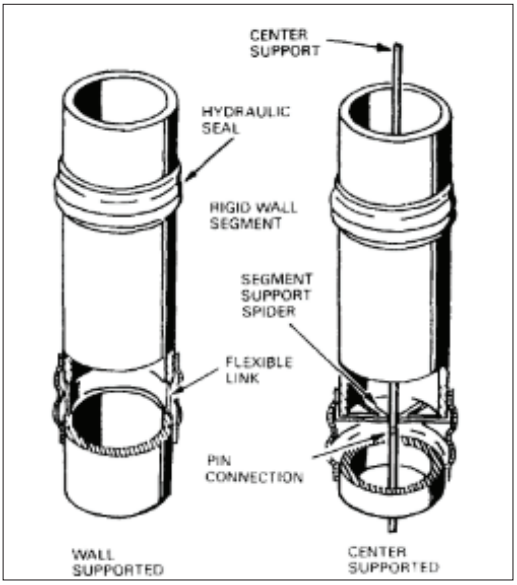

Source: Griffin (1981)

Figure 2.19 Rigid Wall CWP Concept

2. Floating Platform

In the OTEC system, especially in offshore plants, floating platforms function to house all the system equipment used to produce electrical energy (Gava et al., 1978). The floating platform structure is designed to be self-stabilizing even when exposed to external forces due to waves and wind, and to have good seakeeping performance. In addition, the floating platform is also designed to minimize the stress caused by the connection between the system and the CWP.

The floating platform structure is designed according to the size of the plant to be made, so that all equipment can be accommodated without compromising the safety of the structure. In addition, the sea condition in which it operates is also an important consideration. Throughout its development, OTEC, especially on floating platforms, has had many types of designs. One of the simplest is the rectangular shape as found in the Mini OTEC plant as shown in Figure 2.17b. As an alternative to the quadrilateral design on the Mini OTEC, a spar buoy design was proposed by Lockheed Martin. The design was primarily of reinforced-concrete construction, and the cold-water pipe reaches 460 m depth, as shown in Figure 1.20 (Dugger et al., 1975).

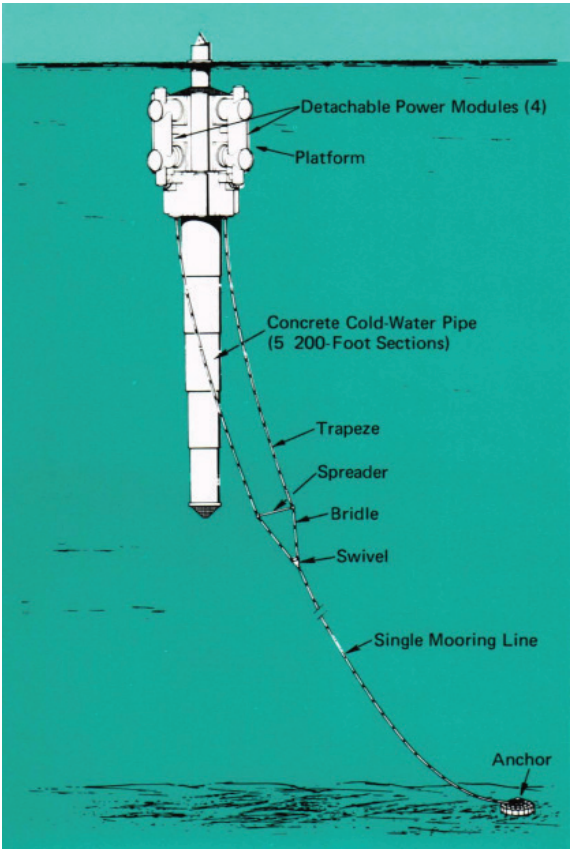

Source: Dugger et al. (1975)

Figure 2.20 Spar Type OTEC Plant by Lockheed Martin

In addition to the type of cycle and plant size, the location of the floating platform is also an influential variable. To withstand strong ocean currents at its site, the University of Massachusetts designed a floating platform using the basic design of a submerged catamaran. Another platform design proposed by Johns Hopkins University's Applied Physics Laboratory uses ship-like propulsion to move the floating OTEC plant across the Pacific and Atlantic Oceans in search

of the desired temperature differential. The hull is planned to be approximately 60 m (Dugger & Francis, 1977; Sasscer & Ortabasi, 1979). To withstand severe wind and wave conditions, Dr. Alfred Lee also proposed an OTEC platform based on the honeycomb concrete framing system as shown in Figure 2.21.

Source: Wang and Wang (2015)

Figure 2.21 Honeycomb Concrete Framing System Based OTEC Plant

Another development related to OTEC floating platforms have been carried out in Japan by considering the design of the ship surface as well as the design of the submerged cylinder. It is designed to withstand the rough sea of Japan. Calculations on the platform design were made with the maximum wind speed of 60 m/s, a current at sea level of 2 knots, and a wave height of 18.5 m (Kamogawa, 1980).

Srinivasan proposed a floating structure called J-Spar, shown in Figure 2.22. This configuration allows the condenser to be located at sea depth. The J-Spar in this design uses welded tubular sections like a conventional jacket structure. The deck section has an eight-foot base

on the bottom. The turbine and generator are placed on the deck, as shown in Figure 2.23. A buoyancy capsule is added to the structure to keep it afloat. As designed, the J-spar is the simplest floating platform design and fabrication process among spar designs. In addition, the J-spar configuration is naturally unaffected by whirlpools caused by underwater currents. Additionally, the suspended cold water pipe configuration makes this installation configuration more stable (Srinivasan, 2009).

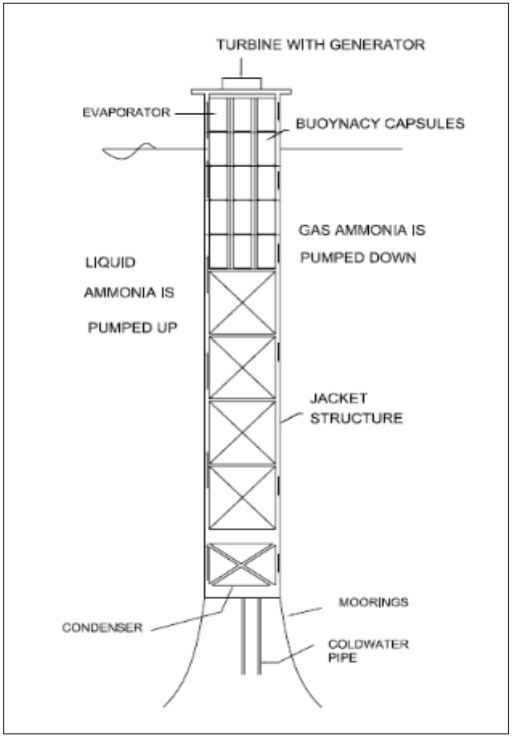

Source: Srinivasan (2009)

Figure 2.22 J-Spar Design

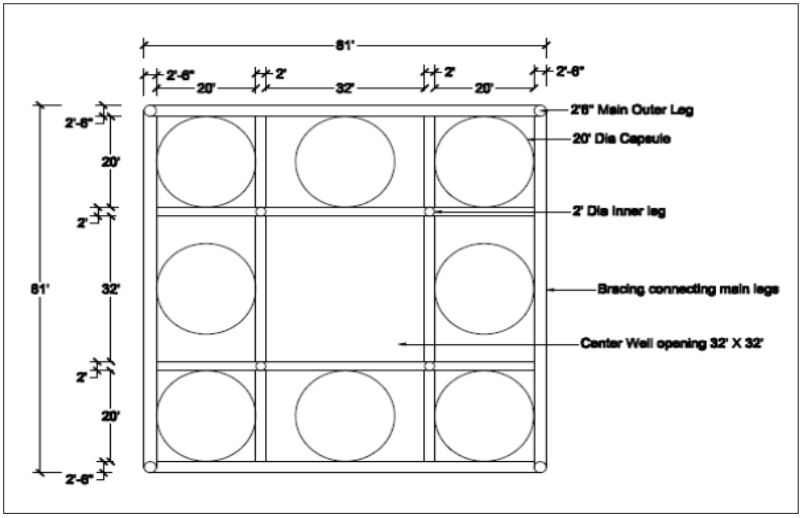

Source: Srinivasan (2009)

Figure 2.23 Cross Sectional of J-Spar Platform Configuration

In addition to J-Spar, the strain-based foot concept can also be used as an alternative for offshore OTEC facilities. This design uses an artificial seabed at a sufficient depth from the actual seabed to reinforce additional systems on the OTEC platform. The artificial seabed consists of a plate structure with a mooring system. In addition, a tensile-based foot system was created and connected to all four corners of the artificial seabed. With this system, condensers can be placed at a depth of around 610 m below sea level. Placing the condenser far below sea level can increase condenser efficiency due to cooler seawater temperatures (Srinivasan, 2009).

The condenser used can also be larger depending on the space available in the clamping base. In addition, the length of the chilled water pipe can be reduced. Another configuration of the tension leg platform is to replace the tension leg platform with a semi-submersible vessel in the OTEC CWP. The mooring system is replaced by a mooring system that allows the semi-submersible to move around. A dynamic positioning system with disconnectable risers is used on the semi-submersible so that the floating plant can be moved in case

of adverse weather conditions. The platform with semi-submersible replacement can be seen in Figure 2.24 (Srinivasan, 2009).

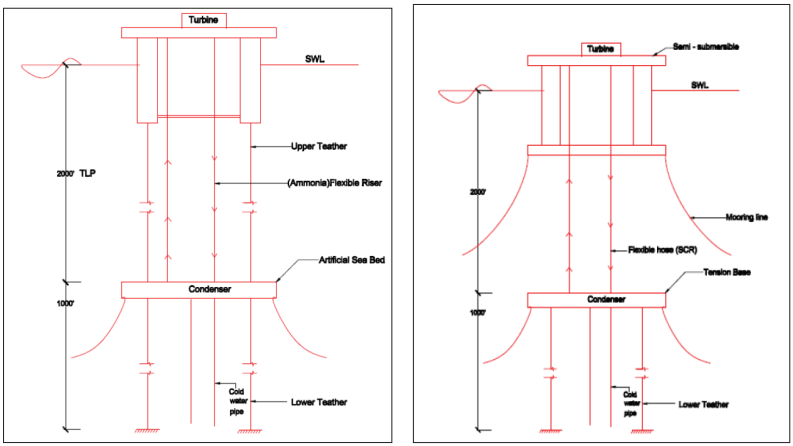

Source: Srinivasan (2009)

Figure 2.24 Cross sectional of J-Spar platform configuration

Another platform being considered for use in the OTEC system is a platform with a reinforced concrete honeycomb frame system. By integrating precast concrete cylindrical components with a top and bottom slap and side wall on the outside of the platform, this platform is considered suitable as a support for OTEC system containers and other components. As an example, the platform application system is the use of a concrete island drilling system (CIDS) in the process of oil exploration and drilling in the US and Russia, precisely in the Arctic Circle area, where the main part for the ice impact resistance on the CIDS platform is the honeycomb module. Where with the use of a honeycomb framing system in the OTEC plant, there will be a large space without columns, so there can be a large and flexible space without obstacles that can be used for an organized and efficient equipment layout. Another research by Adiputra and Utsunomiya (2018) proposed a floating structure design for an OTEC power plant with a capacity of 100 MW. The design of the plant ship proposed

by is to use a commercial oil tanker, which is then converted into an OTEC power ship.

D. OTEC Environmental Impact

OTEC is renewable and does not produce pollutants because it does not require the combustion of fuel to generate electricity (Ma et al., 2022). Further analysis is conducted to determine whether there is an impact on the environment, either positive or negative. Positive impacts are generally in the form of byproducts, as shown in Figure 2.25. Kobayashi et al. (2001) describe several byproducts that can be utilized from the multi-OTEC plant. The development of desalination with surface water sources can be utilized in ocean mineral water, potable water, and hydrogen. Meanwhile, the reuse of deep ocean water (DOW) obtained from certain depth depending on the site location can be used for aquaculture activities, food production, and lithium extraction since the deep ocean water rich with nutrients.

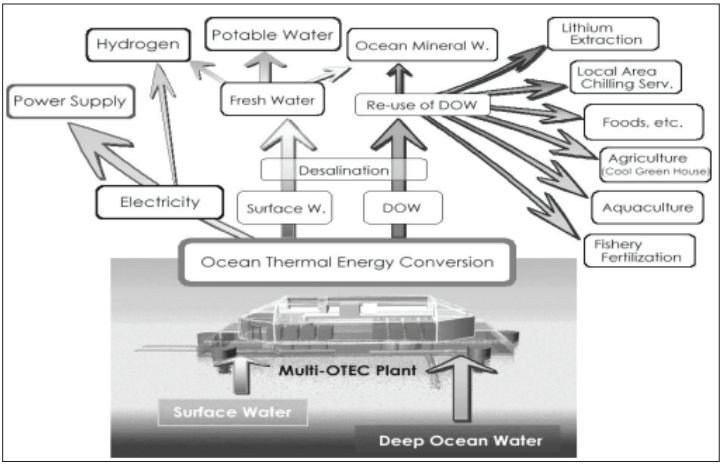

Source: Kobayashi et al. (2001)

Figure 2.25 Benefit from Multi-OTEC Plant

Koto and Negara (2016) state that at a scale of 1 MW, OTEC can produce 4,500 m^3/day of fresh water and can meet the water needs of 20,000 people. Research conducted by Saga University shows that by developing a flash spray system, 100 MW OTEC can produce 1 million m^3/day of water (Kobayashi et al., 2001; Chan et al., 2020). In his research, Kobayashi et al. (2001) stated that only about 1% of raw seawater was desalinated as fresh water, or around 10,000 m^3/day with 1MW OTEC approximately. In addition, freshwater can be converted into several other forms, such as hydrogen, potable water, and seawater mineral water. In the case of hydrogen production, this is a major discovery that can change industrial usage habits from fossil fuels to environmentally friendly hydrogen.

Freshwater produced by the OTEC cycle could also be processed into potable water. This development can reduce the clean water crisis, where a study conducted by Ma et al. (2023) provides data that 1 MW OTEC can provide 2.28 million liters of potable water. This will certainly be mutually beneficial as coastal areas are generally OTEC development areas and areas that often lack fresh water (Welsh & Bowleg, 2022). In addition to the production of seawater, the mineral content and low levels of pollutants in DOW are also used for aquaculture or mariculture activities. DOW was used in regard that it contains almost no contaminated or disease-carrying organisms. A shared system between OTEC and aquaculture could reduce pumping costs. Besides, DOW OTEC has several advantages, such as high-water quality, elevated levels of inorganic nutrients, and the ability to reduce water pumping costs due to OTEC (Mencher et al., 2009). Mencher et al. (2009) used DOW to determine the biological effects on edible seaweed using OTEC in Hawaii. The results of his experiments showed that the edible seaweed developed was of the same quality as high-quality Japanese edible seaweed in a short growth period (3–4 weeks).

Cold seawater left over from OTEC can also be used to support the cooling system in a building (Prawira et al., 2017). In an open-cycle OTEC system, the cold seawater output from the condenser can be used for the air conditioning system. Koto (2016) estimates that the use of air conditioning systems by utilizing the remaining DOW

of the OTEC system can be applied on a large scale and reduce the cost of electricity consumption. In addition to meeting the challenge of electricity demand, OTEC can also meet energy demand. In line with Koto, Chan et al. (2020) estimate that the air conditioning of open cycle OTEC can reduce the impact caused by hotels on Cozumel Island, Mexico.

Currently, the use of OTEC has reached the food, cosmetic, and medical markets. In addition to its use in mariculture, DOW OTEC can also be used in the cosmetic and pharmaceutical industries (Arias-Gaviria et al., 2020). In fact, since 2001, it has been documented that Kumejima (a town in Okinawa, Japan) has utilized the potential of DOW to open a new industry, of which approximately 24% is the cosmetic industry (Martin et al., 2022), as shown in Figure 2.26. The seawater interval used ranges from 15 m for surface seawater to 612 m for deep seawater. And each seawater's maximum flow rate is 13,000 m^3/day.

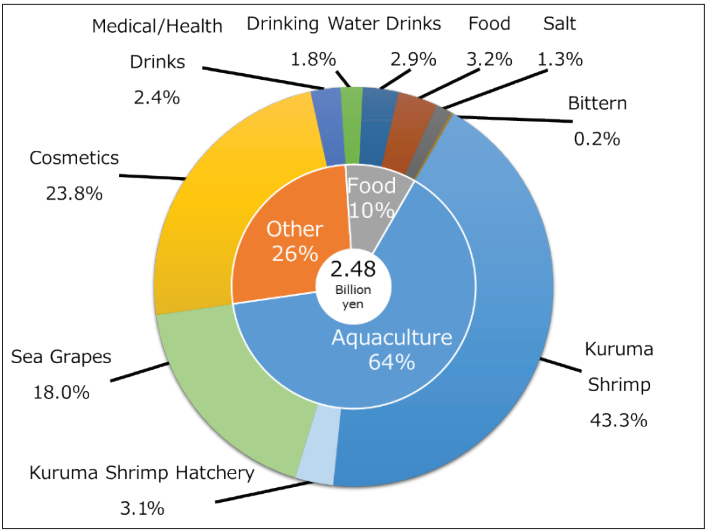

Source: Martin et al. (2022)

Figure 2.26 DOW in Kumejima Town, Okinawa is mainly used for aquaculture (64%).

In the food sector, Kumejima has developed the cultivation of sea grapes through aquaculture. The combination of DOW and surface ocean water is done because of the temperature-sensitive nature of sea grapes. Following the development, an eco-park will be built in Mexico, to meet the growing food demand around Cozumel Island, Mexico (Tobal-Cupul et al., 2022). This will be done by developing OTEC-Offshore Seaweed Aquaculture through the cultivation of *Ulva* spp. as cultivated seaweed for food sources. In 2018, a study conducted by Liu (2018) announced that South China has also started to develop OTECs DOW applications as an alternative energy and food source that can support life.

Figure 2.26 shows that one of the uses of DOW from OTEC development is lithium extraction. This is supported by studies conducted by various researchers (Semmari et al., 2012; Zulqarnain et al., 2023). According to a study conducted by Yoshizuka et al. (2007), lithium as a battery source can be obtained from seawater by ion exchange technique. Among other methods, this method was chosen because it has advantages from an economic and environmental point of view.

Petterson and Kim (2020) mentioned in their study that the use of OTEC side products needs to be further developed, as OTEC development is a form of activity that supports the Sustainable Development Goals (SDGs) as a global success and is a practice of SDG 7 (affordable and clean energy). Suppose by-products—such as desalination, aquaculture, cooling systems, as well as food production, cosmetics, and medical needs—can be developed in addition to lithium extraction, then OTEC development will also contribute to the realization of SDGs 6 (clean water and sanitation), 9 (industrial innovation and infrastructure), and 13 (climate action). In addition, the processing of food, cosmetics, lithium, and medical needs will certainly create jobs, especially for local residents, so that SDGs 1 (no poverty), 2 (zero hunger), 8 (decent work and economic growth), and 11 (sustainable cities and communities) can also be indirectly realized.

However, besides all the advantages and benefits of OTEC development, there are several environmental issues that need attention. As with the choice of working fluid, Jung et al. (2019) compared different types of working fluids such as R32, R125, R134a, R143a, and R410a. According to their study, R134a is the most environmentally friendly type. On the other hand, R32 and R143 are excluded because they are flammable. Working fluids with organic types such as ammonia must also be considered for use because they are toxic substances and can explode under thermodynamically unexpected conditions (Liu et al., 2020). This is certainly very dangerous for the survival of marine flora and fauna, as well as settlements around coastal areas.

E. OTEC Capital

Cost scenario analysis conducted by International Renewable Energy Agency (2014) stated that large-scale OTEC (>100 MW) development is more economically advantageous. In comparison, small-scale OTEC (1–5 MW) requires USD 16,400–35,400/kW, while large-scale (based on feasibility study) ranges from USD 5,000–15,000/kW or even as low as USD 2,500/kW for large-scale floating OTEC. In addition, the cycle selection has a significant difference, where the cost for the open cycle is about USD 2,300/kW higher than the closed cycle (International Renewable Energy Agency, 2014). More detailed cost comparison data is provided based on a study conducted by Muralidharan (2012), which shows a comparison of cost projections with a range of OTEC plant scales in Figure 2.28. Based on Figure 2.27 and Table 2.1, it can be seen that there is a downward trend in capital costs as the capacity of OTEC plants increases.

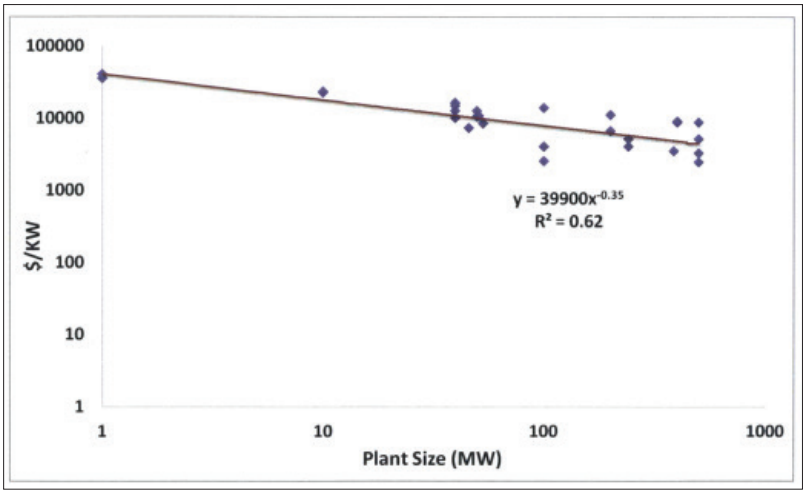

Source: Muralidharan (2012)

Figure 2.27 Trend line of capital costs of OTEC plant for increasing plant sizes. The bigger plant, the cheaper the capital cost.

Table 2.1 Cost Estimates for OTEC and Hybrid OTEC

Size (MW)	Source of LCOE (USD/kWh)[2]				
	(Vega & Asso, 2007; Vega, 2013)	(Energy and Environment Council, 2011)	(Straatman & Van Stark, 2008)	(Upshaw, 2012)	(Muralidharan, 2012)
1–1.35	**0.60–0.94**	**0.51–0.77**			
5	**0.35–0.65**				
10	**0.25–0.45**	**0.19–0.33**			
28				0.13–0.65	
50	**0.08–0.20**	**0.10–0.16**	**0.11–0.32**		
50 (combined with offshore pond)	**0.03–0.05**		0.04–0.06		
100	**0.07–0.18**				**0.19**
200					0.16
400					0.12

Source: International Renewable Energy Agency (2014)

Muralidharan (2012) performed a sensitivity analysis on this comparison and then related the two with a linear equation formula, as shown in Equation (2.3).

$$\text{Capital Cost (\$/kW)} = 39{,}900 \times \text{MW}^{-0.35} \quad (2.3)$$

Based on the trend and the formula, there is a one-fifth reduction in capital cost for each doubling of the OTEC plant. When the capacity of the plant is compared to the capital cost required, the capital cost decreases as the capacity of the OTEC plant increases.

A similar study was also conducted by Vega (2013) which compared OTEC capital costs from various literature as shown in Table 2.2 and Figure 2.28. In the presented data, the capital costs have been converted and adjusted to 2013 costs. When comparing the capital costs between 1.4 MW and 100 MW, the differences reaching about as high as USD 34,000/kW. In contrast, a significant decrease applies to 1.4–10 MW plants. For developing less than 1.4 MW, the decrease is less significant and tends to remains stable. In his research, Vega also formulated a function to determine the capital cost using variable plant capacity in an exponential function, as shown in Equation (2.4).

$$\text{Capital Cost (\$/kW)} = 53{,}160 \times \text{MW}^{-0.418} \quad (2.4)$$

Table 2.2 OTEC Plant Capital Cost Estimates

Plant size (MW-net)	Installed capital cost ($/kW)	Land/Floater	Source
1.4	**41,562**	L	(Vega, 1992)
5	**22,812**	L	(Vega, 2010)
5.3	**35,237**	F	(Vega, 1994)
10	**24,071**	L	(Vega, 1992)
10	**18,600**	F	(Vega, 2010)
35	**12,000**	F	(Vega, 2010)
50	**11,072**	F	(Vega, 1992)
53.5	**8,430**	F	(Vega, 2010)
100	**7,900**	F	(Vega, 2010)

Source: Vega (2013)

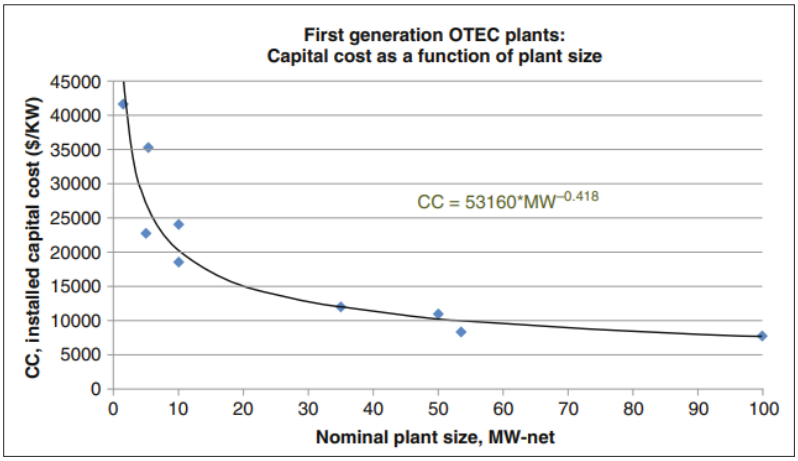

Source: Muralidharan (2012)

Figure 2.28 Capital cost estimated for OTEC plants.

To advance the economic assessment, the levelized cost of electricity (LCOE) must also be estimated in the economic calculation which is one of the parameters used to forecast energy supply and demand (Muralidharan, 2012; Kearney, 2010). As shown in Table 2.3, based on Vega (2013), the LCOE data is amortized with a loan of 8%/15 years and annual inflation of 3%.

The cost of electricity (COE) data presented in Table 2.3 are presented in a graph and compared with the scenario in which the OTEC development is financed by the government with a realistic rate of 4.2%/20 years. In the data comparison shown in Figure 2.29, the COE value can be reduced using the government funding scenario. In addition, the current development of OTEC in different regions is still on a small scale. As can be seen, significant differences occur at the smallest scale, where the difference reaches about 20 cents/kWh. Although the cost difference decreases as the plant capacity increases, the government funding scenario can mitigate and reduce the COE.

Table 2.3 Levelized Cost of Electricity (US-cents/kWh) for CC-OTEC Plants with Capital Costs (CC)

Identifier nominal size (MW)	Capital cost ($/kW)	Operation & maintenance ($M/year)	Repair & replacement cost ($M/year)	Cost of electricity considering capital cost (c/kWh)	Cost of electricity considering operation, maintenance, repair & replacement cost (c/kWh)	Cost of electricity (C/kWh)
1.35	**41,562**	**2.0**	**1.0**	**60**	**33.7**	**94.0**
5	**22,812**	**2.0**	**3.5**	**33**	**17**	**50.0**
10	**18,600**	**3.4**	**7.7**	**26.9**	**16.8**	**44.0**
53.5	**8,430**	**3.4**	**20.1**	**12.2**	**6.7**	**19.0**
100	**7,900**	3.4	36.5	11.4	6	18.0

Source: Vega (2013)

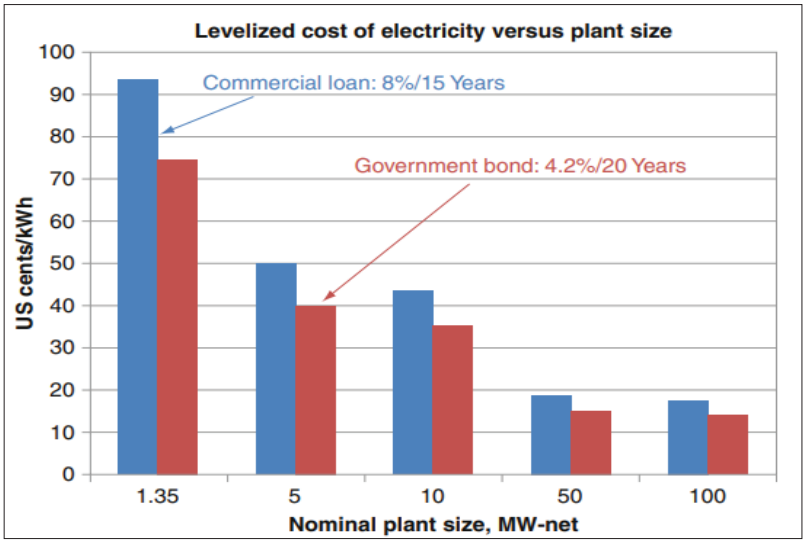

Source: Vega (2013)

Figure 2.29 Cost of Electricity (Capital Cost Amortization + OMR&R Levelized Cost) Production for First-Generation OTEC Plants

Ocean Energy Systems (2015) conducted an economic analysis of ocean energy technologies, including OTEC, through the International Levelized Cost of Energy for Ocean Energy Technologies. The calculation of capital expenditure (CAPEX) and operating expenditure (OPEX) are described in Figures 2.30 and 2.31, respectively. In the CAPEX cost breakdown, there is a difference in cost allocation, where at the 5 MW scale, platforms/moorings have the largest percentage. While at the 100 MW scale, power conversion is the largest contributor to CAPEX, up to 61%. In other cases, as shown in Figure 2.31, maintenance is the largest contributor at 54% in the case of 100 MW OTEC. This is due to the significant amount of power-generating equipment, such as heat exchangers.

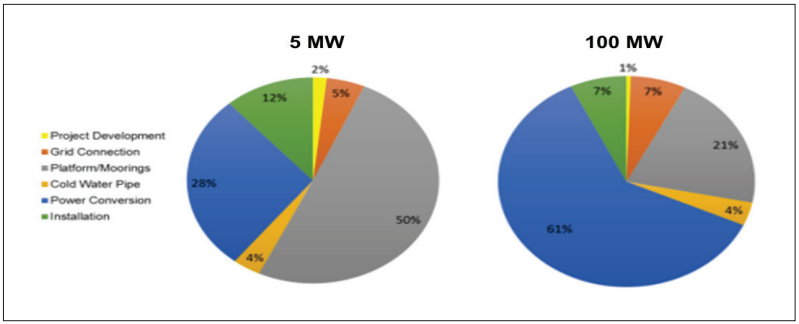

Source: Ocean Energy Systems (2015)

Figure 2.30 CAPEX Cost Breakdown at 5 MW Deployment Scale and 100 MW Deployment Scale

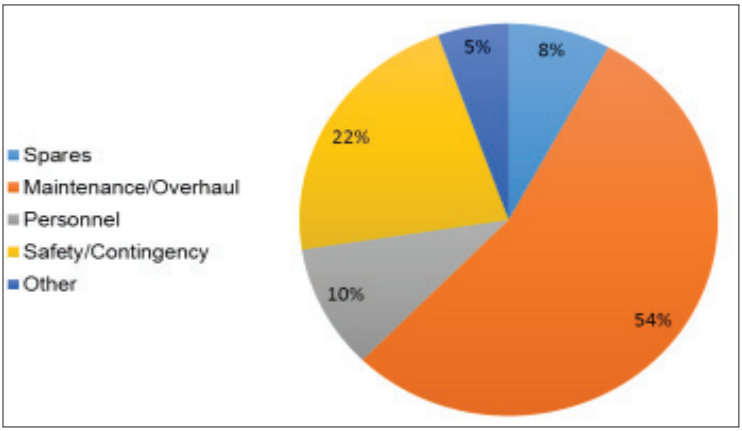

Source: Ocean Energy Systems (2015)

Figure 2.31 Representative OPEX Cost Breakdown for a 100 MW OTEC Plant

Ocean Energy Systems (2015) obtained LCOE by processing plant capacity data and comparing it with LCOE, as shown in Figure 2.32. Similar results are seen in the comparison with capital cost, the comparison with LCOE also shows a decrease in LCOE as the OTEC plant capacity increases.

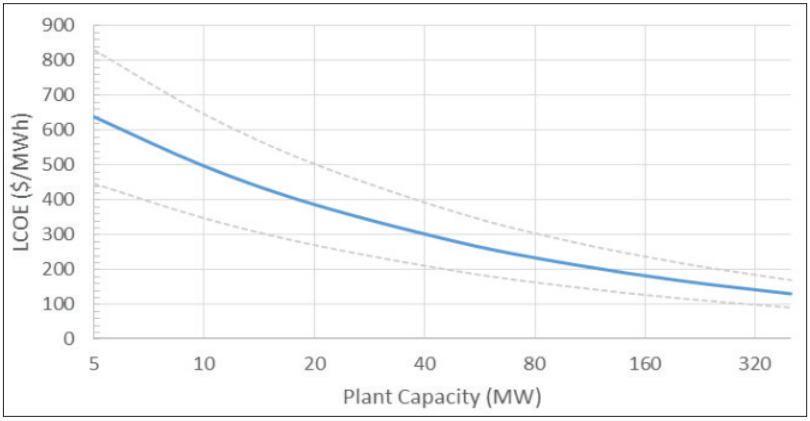

Source: Ocean Energy Systems (2015)

Figure 2.32 LCOE as a Function of Plant Scale

In addition to decreasing LCOE, increasing plant capacity will also affect the distribution of LCOE cost centers, as shown in Figure 2.33. Increasing the capacity from 5 MW to 100 MW will reduce the LCOE from 40% to 80% (Ocean Energy Systems, 2015). This change will shift the LCOE cost breakdown from almost half of the total for platform/mooring to power conversion. This is in line with the study by Muralidharan (2012), where the platform structure and the heat exchange system are the major cost contributors for different types and sizes of OTEC plants, as shown in Figure 2.34.

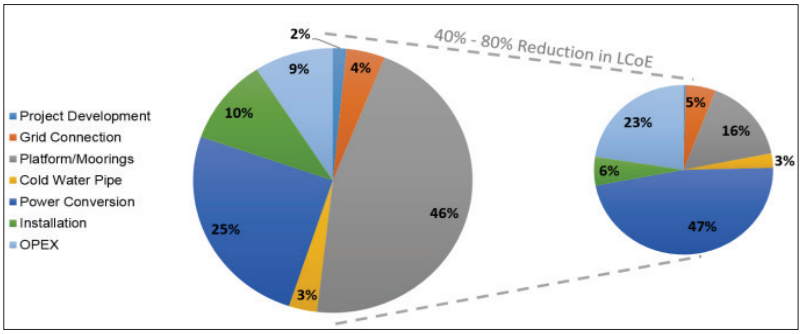

Source: Muralidharan (2012)

Figure 2.33 LCOE Cost Centers for 5MW Plant (left) and 100MW Plant (right)

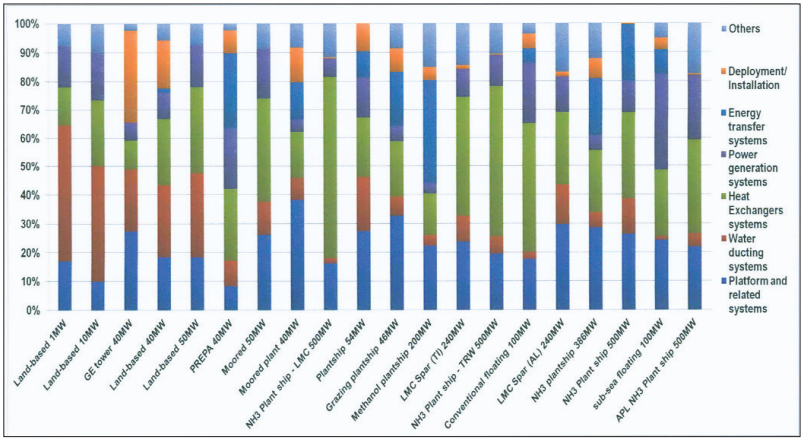

Source: Muralidharan (2012)

Figure 2.34 Proportion of Cost in Historical OTEC Designs

In the feasibility study conducted by Tobal-Cupul et al. (2022) on the OTEC eco-park in Cozumel Island, a comparison of LCOE between OTEC and other types of alternative energy sources was made. Initially, the potential was assessed. From Figure 2.35, it can be seen that OTEC is a stable renewable energy with the highest energy security. The electricity product is the most stable in all four seasons

compared to other energy sources with the energy potential in a range between 45–60 MW.

The LCOE comparison is made by considering the capacity factor (CF) value, as shown in Figure 2.36. The (*) and (**) represent the source of the data, while the circle represent the difference between OTEC plant based on the data. The CF is the ratio of the energy produced in a given period to the energy produced at full capacity in the same period at the same power output. Although the OTEC 60 MW floating plant in Cozumel Island has the highest LCOE, both the OTEC plant in Cozumel Island and the OES has the highest CF of about 90%. The LCOE of OTEC can be reduced by increasing the capacity factor of the plant, as discussed above. The production of byproducts and non-energy needs can also be a solution to reduce the LCOE. Thus, economically wise, the LCOE of OTEC can be reduced, and other economic activities can be formed due to the presence of OTEC.

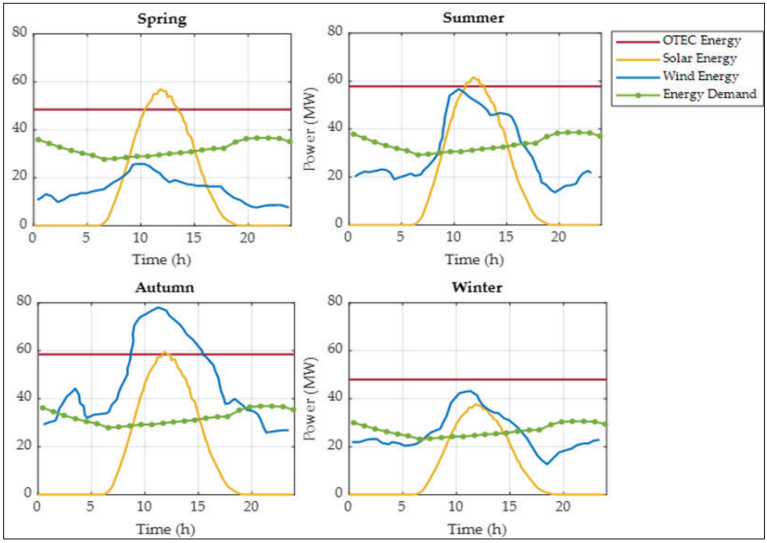

Source: Tobal-Cupul et al. (2022)

Figure 2.35 Comparison of Seasonal Power Generation in Cozumel Island, Mexico: OTEC, Solar and Wind Energies

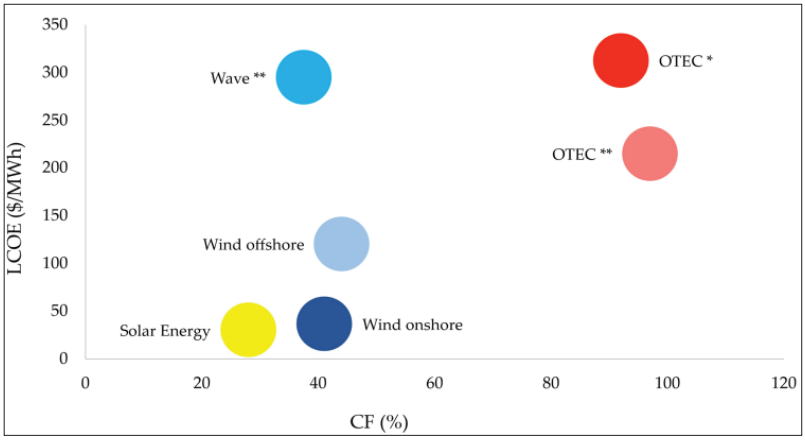

Source: Tobal-Cupul et al. (2022)*, US Energy Information Administration (2022), and Ocean Energy Systems (2018)**.

Figure 2.36 Comparison of the LCOE and CF for OTEC and Other Renewable Energies

F. OTEC in Indonesia

Indonesia has great potential of sea temperature to be exploited for OTEC. This potential can be seen from the high temperature difference between the surface and the deep sea level. As shown in Figure 2.37, the sea temperature difference in the central and eastern regions of Indonesia is 24°C on average. The temperature difference is very suitable for OTEC systems, especially the Rankine cycle, which requires a temperature difference of 15–25°C to achieve a thermal efficiency of about 3% (Nakaoka & Uehara, 1988).

To corroborate the temperature difference map as shown in Figure 2.37, several researchers have investigated the potential of OTEC in Indonesia. Research by Sinuhaji (2015) on the potential of OTEC in Bali shows that a plant with a capacity of 125 kW and a temperature difference of about 20.5°C can produce a net power of 69.4 kW, with a cycle efficiency of 3.1%. Based on the study of Syamsuddin et al. (2015), as shown in Table 2.4, the average value of Carnot cycle efficiency for OTEC systems in several locations in Indonesia is more

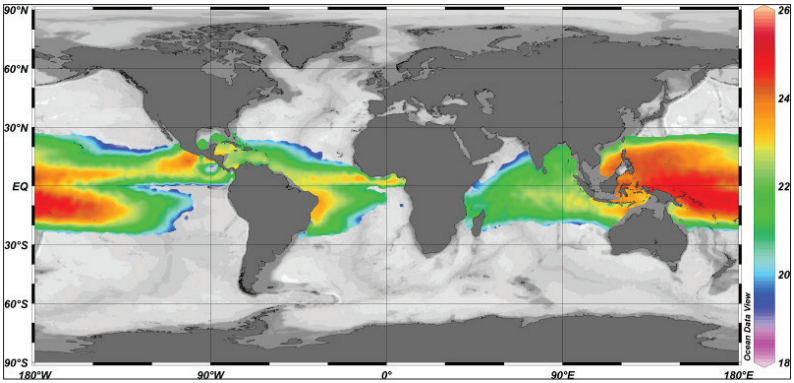

Source: Rajagopalan and Nihous (2013)

Figure 2.37 Mean Temperature Difference between Water Depths of 20 m and 1000 m

than 0.75. This shows the great potential of OTEC in Indonesia, given the average Carnot cycle values in several of these locations.

Several researchers have also conducted investigations on OTEC in Indonesia. Setiawan et al. (2017) optimized the Kalina closed cycle with ammonia working fluid to be implemented in Mamuju, West Sulawesi. The optimization was carried out by adding a flat plate solar collector with an area of approximately 6,023 x 106 m^2, as shown in Figure 2.38. The solar collector is used to heat the warm seawater to 33.5°C before it enters the evaporator. It is concluded that for plants with a capacity of 33 MWe and an efficiency of 7.1%, the capacity can be increased to 144,155 MWe with an efficiency of 9.54% by adding a flat plate solar collector. However, the effects of the installation of the flat plate solar collector on LCOE had not been included in analysis.

Table 2.4 Carnot Efficiency System OTEC in Several Locations in Indonesia

Location	Tw (°C)	Tc (°C)	ΔT	Depth (m)	Carnot Efficiency
South Kalimantan	28.82	7.71	21.11	500	0.73
North Sulawesi	29.22	7.44	21.78	500	0.74
Timur Strait	28.83	6.72	22.11	600	0.76
Makassar Strait	28.83	6.72	22.11	600	0.76
South Sulawesi	28.47	6.18	22.29	700	0.78
West Papua	28.16	6.76	21.40	600	0.75
Morotai Sea	28.47	6.82	21.65	600	0.76

Source: Syamsuddin et al. (2015)

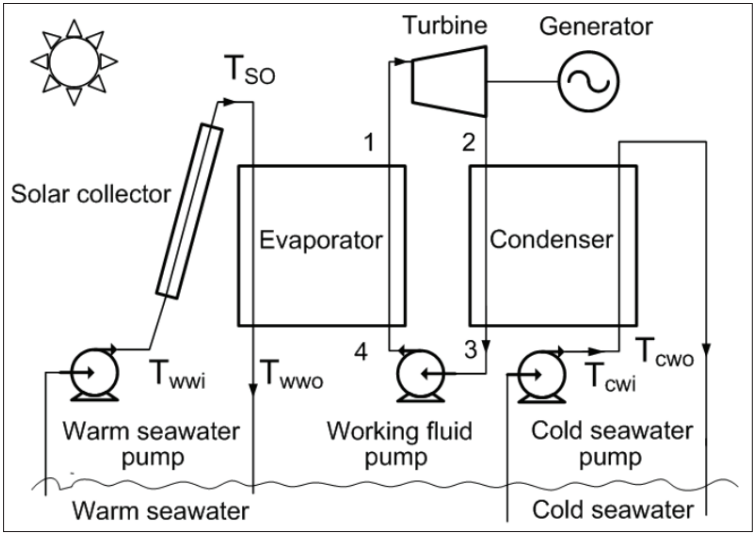

Source: Setiawan et al. (2017)

Figure 2.38 OTEC Plant with a Flat-Plate Solar Collector Design

Adiputra and Utsunomiya (2018) made a design of a 100 MW OTEC power plant for Mentawai Island, Indonesia, using the basic Suezmax oil tanker type as the plant ship. It was concluded that the Suezmax oil tanker ship is sufficient to accommodate the 100 MW

OTEC power plant. Adiputra et al. (2020) set some limitations as considerations to determine whether certain cases are acceptable or not. The limitations that have been taken into consideration are the space available, the allowable weight, and the net power output. Considering the fixed variables as well as the limitations set, it was concluded that a Suezmax-type oil tanker with a seawater displacement of 3 m/s is the most appropriate type. The outline of the ship is drawn with reference to the book "Principle of Naval Architecture," with the same size tendency in the parameters used. The drawing is shown in Figure 2.39. The main dimensions of the ship are given in Table 2.5.

Table 2.5 Suezmax Main Dimension of the Plant Ship

Parameter	Value
Type	Suezmax
Length between perpendicular (m)	275
Length overall (m)	285
Breadth (m)	50
Height (m)	30
Draft (m)	17
Coefficient block	0.945
Tonnage (ton)	200000

Source: Adiputra et al. (2020)

Regarding the main dimension of the required CWP, Adiputra and Utsunomiya (2019) stated that to generate 100 MW-net of energy, the OTEC CWP required a configuration of 800 m in length and a 12 m diameter pipe connected to the plant ship. With this specified configuration, the connection between the OTEC CWP and the platform will be the main support for the OTEC CWP component (Adiputra et al., 2020). In further research, based on the manufacture limitation, Adiputra estimated that, by considering recent manufacture capability of the related industry, the maximum diameter pipe that can be attached to the platform is a 3 m-diameter pipe (Adiputra & Utsunomiya, 2021).

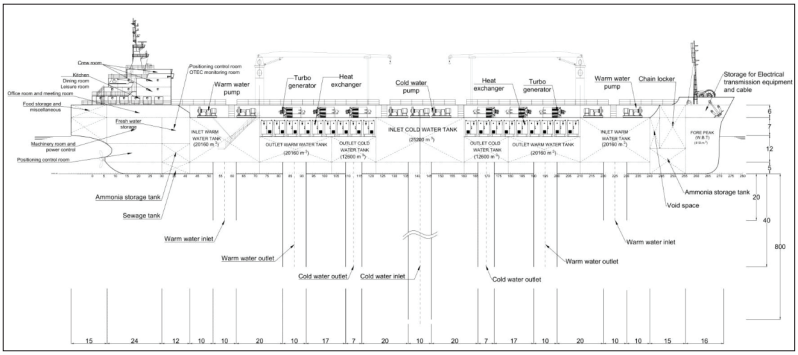

Source: Adiputra et al. (2020)

Figure 2.39 Layout of 100 MW net of OTEC Plant Ship Design

Adiputra and Utsunomiya (2021) are attempting to design a CWP on a commercial scale, focusing on the effects caused by the internal flow of the pipeline which may cause instability. The analyses carried out in the design process also aimed to select suitable materials for the pipe, the configuration of the pipe joint and floating platform, and the selection of ballast at the inlet end of the pipe, through numerical and analytical analysis. It was found that the most suitable material for the OTEC CWP is fiber reinforced polymer (FRP), considering that FRP tends to be lightweight, strong, and can withstand high levels of stress. The pinned joint installation configuration is also the best installation configuration as it has the least stress at the joint but tends to remain stable. The addition of clump weight was also considered as it helps to stabilize the pipe (Adiputra & Utsunomiya, 2021).

Currently, Indonesia is pursuing a goal of generating 52% of its electricity from new renewable energy sources by 2040. Based on the report of the Special Task Force for Upstream Oil and Gas Business Activities (SKK Migas), as of March 2021, there were 634 offshore oil and gas platforms in Indonesia, of which 100 were no longer operational. Hence, the offshore oil and gas platform can be used to become a prospective floating platform OTEC power plant.

Additionally, a pilot project of 1 MW-net OTEC platform had been successfully built which encouraged the OTEC development (Petterson & Kim, 2020). As a country with huge OTEC potential of about 4,000 GW, it is a big opportunity for Indonesia to accomplish net zero-emission in 2060 by establishing a strength collaboration between the government, industries, researchers, and universities to work on OTEC. The government is to establish regulations for providing a long-term investment and initiate the pilot projects for development activities. The national and private companies work on the OTEC supply chain. The research body conducted investigations on the technology advancement and the universities produced human resources with intellection capital on OTEC.

Despite its high potential in Indonesia, OTEC power plant also possess some environmental damage potential. OTEC power plants, like other types of power plants, can generate noise. Noise measurements at the 1 MW OTEC plant in Keahole, Hawaii, showed that the noise generated by the seawater pump, the plant's main noise source, did not exceed 10 dB, although this could increase if the plant were larger (Spellman, 2016). The discharged water could potentially pose a threat to the environment. A 100 MW plant would require 10–20 billion gallons of warm surface water and cold water per day (NOAA, 2010). Discharging water with varying temperatures and nutrient levels can be harmful to the environment and the species that live in it. The extraction of minerals from seawater could potentially cause an imbalance in the marine ecosystem. Before OTEC power plants are commercialized in Indonesia, their potential environmental impact needs to be further investigated.

G. Closing

Based on the type of cycle, OTEC systems can be divided into three main categories: closed-cycle, open-cycle, and hybrid cycle. Closed-cycle OTEC is based on the Rankine cycle with a pure working fluid operating under isolated conditions. Open-cycle OTEC operates under vacuum conditions using warm seawater as the working fluid

and can produce desalinated water. The hybrid cycle OTEC uses a combination of open and closed cycles to produce working fluid vapor, which is then distilled and used as potable water.

In the OTEC cycle system, the turbine is the main component that can convert thermal energy into mechanical energy and then into electrical energy by the generator. In general, the OTEC cycle uses radial flow turbines. This is because radial flow turbines still have high efficiency even though the mass flow of fluid is minimal.

In the offshore OTEC plant, there are several proposed potential models, such as the tanker model, J-spar, and tension-based system. The OTEC's cold water pipe (CWP) is a critical component of the OTEC platform system. The CWP is used to discharge cold seawater required for the OTEC cycle. CWP made of fiber reinforced polymer (FRP) and sandwich wall structure in pinned joint at the top is the most preferable configuration.

The development of OTEC offers several co-products, such as the development of water desalination by producing fresh water, drinking water, and hydrogen from surface seawater. Meanwhile, the use of deep-sea water, which is highly nutritious and low in pollutants, can be used for aquaculture, food production, cosmetics, and lithium extraction. However, environmental impacts such as the use of working fluids that have the potential to damage the environment need to be examined. When used optimally, OTEC development supports many aspects of the SDGs goals.

The capital cost and LCOE of OTEC show a decreasing trend as OTEC plant capacity increases. Although the LCOE value of OTEC is high compared to other types of renewable energy, the CF value of OTEC is the highest. The potential for by-product development can be a solution to reduce the LCOE and create the potential for economic activities.

The commercialization of OTEC power plants in Indonesia can be the key to achieving Indonesia's renewable energy target by 2040. The development of OTEC in Indonesia is currently underway. With all the potential that exists, it is only a matter of time before

a commercial scale OTEC power plant can be realized. However, without the impetus and acceleration, OTEC power plants cannot be commercialized before 2040.

The OTEC power plant has great potential in Indonesia. The environmental damage that may occur in Indonesia has not been thoroughly studied. This must be an important consideration in the development process of the OTEC power plant. In this way, the journey towards renewable energy does not sacrifice the safety of the ecosystem.

Reference

Adiputra, R., & Utsunomiya, T. (2018). Design optimization of floating structure for a 100 MW-Net Ocean Thermal Energy Conversion (OTEC) power plant. In *37th International Conference on Ocean, Offshore and Arctic Engineering*, 3, (1–9). The American Society of Mechanical Engineers. https://doi.org/10.1115/OMAE2018-77539

Adiputra, R., & Utsunomiya, T. (2019). Stability based approach to design cold-water pipe (CWP) for ocean thermal energy conversion (OTEC). *Applied Ocean Research*, *92*, 101921. https://doi.org/10.1016/j.apor.2019.101921

Adiputra, R., & Utsunomiya, T. (2021). Linear vs non-linear analysis on self-induced vibration of OTEC cold water pipe due to internal flow. *Applied Ocean Research*, *110*, 102610. https://doi.org/10.1016/j.apor.2021.102610

Adiputra, R., Utsunomiya, T., Koto, J., Yasunaga, T., & Ikegami, Y. (2020). Preliminary design of a 100 MW-net ocean thermal energy conversion (OTEC) power plant study case: Mentawai island, Indonesia. *Journal of Marine Science and Technology (Japan)*, *25*(1), 48–68. https://doi.org/10.1007/s00773-019-00630-7

Alawadhi, K., Alhouli, Y., Ashour, A., & Alfalah, A. (2020). Design and optimization of a radial turbine to be used in a rankine cycle operating with an OTEC system. *Journal of Marine Science and Engineering*, *8*(11), 855. https://doi.org/10.3390/jmse8110855

Arias-Gaviria, J., Osorio, A. F., & Arango-Aramburo, S. (2020). Estimating the practical potential for deep ocean water extraction in the Caribbean. *Renewable Energy*, *150*, 307–319. https://doi.org/10.1016/j.renene.2019.12.083

Avery, W. H., & Wu, C. (1994). *Renewable energy from the ocean: A guide to OTEC*. Oxford University Press.

Aydin, H., Lee, H. S., Kim, H. J., Shin, S. K., & Park, K. (2014). Off-design performance analysis of a closed-cycle ocean thermal energy conversion system with solar thermal preheating and superheating. *Renewable Energy*, *72*, 154–163. https://doi.org/10.1016/j.renene.2014.07.001

Bharathan, D., Green, H. J., Link, H. F., Parsons, B. K., Parsons, J. M., & Zangrando, F. (1990). *Conceptual Design of an Open-Cycle Ocean Thermal Energy Conversion Net Power-Producing Experiment (OC-OTEC NPPE)* [Technical Report]. U.S. Department of Energy, Office of Scientific and Technical Information. https://doi.org/10.2172/6625364

Calleja-Agius, J., England, K., & Calleja, N. (2021). The effect of global warming on mortality. *Early Human Development*, *155*, 105222 https://doi.org/10.1016/j.earlhumdev.2020.105222

Chan, E. C. C., Tun, M. F. S., Graniel, J. F. B., & Acevedo, E. C. (2020). Environmental impact assessment of the operation of an open cycle OTEC 1MWe power plant in the Cozumel Island, Mexico. In A. S. Kim & H.-J. Kim (Eds.), *Ocean Thermal Energy Conversion (OTEC)* (p. ch. 8). IntechOpen. https://doi.org/10.5772/intechopen.91179

Chen, F., Liu, L., Peng, J., Ge, Y., Wu, H., & Liu, W. (2019). Theoretical and experimental research on the thermal performance of ocean thermal energy conversion system using the rankine cycle mode. *Energy*, *183*, 497–503. https://doi.org/10.1016/j.energy.2019.04.008

Chen, Y., Liu, Y., Liu, W., Ge, Y., Xue, Y., & Zhang, L. (2022). Optimal design of radial inflow turbine for ocean thermal energy conversion based on the installation angle of nozzle blade. *Renewable Energy*, *184*, 857–870. https://doi.org/10.1016/j.renene.2021.12.016

Chen, Y., Liu, Y., Yang, W., Wang, Y., Zhang, L., & Wu, Y. (2021). Research on optimization and verification of the number of stator blades of kW ammonia working medium radial flow turbine in ocean thermal energy conversion. *Journal of Marine Science and Engineering*, *9*(8), 901. https://doi.org/10.3390/jmse9080901

Curzon, F. L., & Ahlborn, B. (1975). Efficiency of a Carnot engine at maximum power output. *American Journal of Physics*, *43*(1), 22–24. https://doi.org/10.1119/1.10023

Dugger, G. L., & Francis, E. J. (1977). Design of an ocean thermal energy plant ship to produce ammonia via hydrogen. In *International Journal of Hydrogen Energy* (Vol. 2). Pergamon Press.

Dugger, G. L., Olsen, H. L., Shippen, W. B., Francis, E. J., & Avery, W. H. (1975). Ocean thermal power plants. *Johns Hopkins APL Technical Digest*, *14*, 2–20. https://secwww.jhuapl.edu/techdigest/Content/techdigest/pdf/APL-V14-N01/APL-14-01-Dugger.pdf

US Energy Information Administration. (2022). *Levelized costs of new generation resources in the annual energy outlook 2022*. https://www.eia.gov/outlooks/aeo/pdf/electricity_generation.pdf

Esteban, M., & Leary, D. (2012). Current developments and future prospects of offshore wind and ocean energy. *Applied Energy*, *90*(1), 128–136. https://doi.org/10.1016/j.apenergy.2011.06.011

Ganic, E. N., & Moeller, L. (1980). Performance study of an OTEC system. *Applied Energy*, 6(4), 289–299. https://doi.org/10.1016/0306-2619(80)90019-7

Gava, P., Bozzo, G. M., & Paruzzolo, A. (1978, 8–11 May). *A feasible concept for an integrated OTEC floating structure* [Paper Presentation]. Offshore Technology Conference, Texas, United States of America. https://doi.org/https://doi.org/10.4043/3334-MS

Griffin, O. M. (1981). *OTEC cold water pipe design for problems caused by vortex-excited oscillations. Ocean Engineering, 8*(2), 129–209. https://doi.org/10.1016/0029-8018(81)90023-8

Hernández-Romero, I. M., Zavala, V. M., Flores-Tlacuahuac, A., Nápoles-Rivera, F., Fuentes-Cortés, L. F., & Esquivel-Patiño, G. G. (2022). Multi-objective optimization of an open-cycle, ocean thermal energy conversion system with desalinization. *Chemical Engineering and Processing - Process Intensification*, *179*. https://doi.org/10.1016/j.cep.2022.109091

Herrera, J., Sierra, S., & Ibeas, A. (2021). Ocean thermal energy conversion and other uses of deep sea water: A review. *Journal of Marine Science and Engineering, 9*(4), 356. https://doi.org/10.3390/jmse9040356

Hisamatsu, R., & Utsunomiya, T. (2022). Coupled response characteristics of cold water pipe and moored ship for floating OTEC plant. *Applied Ocean Research*, *123*, 103151. https://doi.org/10.1016/j.apor.2022.103151

IEA. (2020). *Global energy review 2019: The latest trends in energy and emissions in 2019*. OEDC Publishing. https://doi.org/10.1787/90c8c125-en

IEA. (2021). *Electricity market report, July 2021*. OECD Publishing. https://doi.org/10.1787/f4044a30-en

Ikegami, Y., & Bejan, A. (1998). On the thermodynamic optimization of power plants with heat transfer and fluid flow irreversibilities. *Journal of Solar Energy Engineering, 120(2)*, 139–144. https://doi.org/10.1115/1.2888057

International Renewable Energy Agency. (2014). *Ocean Therman Energy Conversion* [Technology Brief]. International Renewable Energy Agency. https://www.irena.org/-/media/Files/IRENA/Agency/Publication/2014/Ocean_Thermal_Energy_V4_web.pdf?rev=f8b271abc44549f78f68c25ad1380d9e

Johnson, D. H. (1983). The exergy of the ocean thermal resource and analysis of second-law efficiencies of idealized ocean thermal energy conversion power cycles. *Energy, 8(12)*, 927–946. https://doi.org/10.1016/0360-5442(83)90092-0

Jung, H., Jo, J., Chang, J., & Lee, S. (2019). Experimental study on combined ocean thermal energy conversion with waste heat of power plant. *KEPCO Journal on Electric Power and Energy*, *5*(3), 215–222. https://doi.org/10.18770/KEPCO.2019.05.03.215

Kalina, A. I. (1983). *Combined cycle and waste heat recovery power systems based on a novel thermodynamic energy cycle utilizing low-temperature heat for power generation*. American Society of Mechanical Engineers. http://asmedigitalcollection.asme.org/GT/proceedings-pdf/JPGC1983-GTPapers/79368/V001T02A003/2513296/v001t02a003-83-jpgc-gt-3.pdf

Kalina, A. I. (1984). Combined-cycle system with novel bottoming cycle. *Journal of Engineering for Gas Turbines and Power, 106(4)*, 737–742. https://doi.org/10.1115/1.3239632

Kamogawa, H. (1980). *OTEC research in Japan* (Vol. 5). Pergamon Press Ltd.

Kearney, D. (2010, March 23). *EIA's outlook through 2035* [Presentation]. Annual Energy Outlook 2010, Washington DC, USA. https://www.stb.gov/wp-content/uploads/files/docs/railEnergyTransportationAdvisoryCommittee/EIA%20AEO%202010.pdf

Kim, A. S., Kim, H. J., Lee, H. S., & Cha, S. (2016). Dual-use open cycle ocean thermal energy conversion (OC-OTEC) using multiple condensers for adjustable power generation and seawater desalination. *Renewable Energy*, *85*, 344–358. https://doi.org/10.1016/j.renene.2015.06.014

Kobayashi, H., Jitsuhara, S., & Uehara, H. (2001). The present status and features of OTEC and recent aspects of thermal energy conversion technologies. *National Maritime Research Institute, Japan*. https://newsroom.prkarma.com/assets/newsroom/documents/555.svrybz5k.pdf

Koto, J. (2016). Potential of Ocean Thermal Energy Conversion in Indonesia. *International Journal of Environmental Research & Clean Energy, 4(1)*, 1–7. https://tethys.pnnl.gov/sites/default/files/publications/Koto_et_al_2016.pdf

Koto, J., & Negara, R. B. (2016). 10 MW Plant Ocean Thermal Energy Conversion in Morotai Island, North Maluku, Indonesia. *Journal of Subsea and Offshore -Science and Engineering-*, *8*, 7–14. https://isomase.org/JSOse/Vol.8 Dec 2016/8-2.pdf

Lee, H. S., Yoon, J. I., Son, C. H., Ha, S. J., Seol, S. H., Ye, B. H., Kim, H. J., & Jung, G. J. (2015). Efficiency enhancement of the ocean thermal energy conversion system with a vapor-vapor ejector. *Advances in Mechanical Engineering*, 7(3), 1–10. https://doi.org/10.1177/1687814015571036

Link, H. F., & Parsons, B.K. (1986). Potential of proposed open-cycle OTEC experiments to achieve net power. Solar Energy Research Institute. In *OCEANS*, *86*, 207–212. IEEE. https://www.nrel.gov/docs/legosti/old/2965.pdf

Liu, C. C. K. (2018). Ocean thermal energy conversion and open ocean mariculture: The prospect of Mainland-Taiwan collaborative research and development. *Sustainable Environment Research*, *28*(6), 267–273.. https://doi.org/10.1016/j.serj.2018.06.002

Liu, W. M., Chen, F. Y., Wang, Y. Q., Jiang, W. J., & Zhang, J. G. (2011). Progress of closed-cycle OTEC and study of a new cycle of OTEC. *Advanced Materials Research*, *354–355*, 275–278. https://doi.org/10.4028/www.scientific.net/AMR.354-355.275

Liu, W., Xu, X., Chen, F., Liu, Y., Li, S., Liu, L., & Chen, Y. (2020). A review of research on the closed thermodynamic cycles of ocean thermal energy conversion. *Renewable and Sustainable Energy Reviews*, *119*, 109581. https://doi.org/10.1016/j.rser.2019.109581

Ma, Q., Huang, J., Gao, Z., Lu, H., Luo, H., Li, J., Wu, Z., & Feng, X. (2022). Performance improvement of OTEC-ORC and turbine based on binary zeotropic working fluid. *International Journal of Chemical Engineering*, 2023. https://doi.org/10.1155/2023/8892450

Ma, Q., Zheng, Y., Lu, H., Li, J., Wang, S., Wang, C., Wu, Z., Shen, Y., & Liu, X. (2022). A novel ocean thermal energy driven system for sustainable power and fresh water supply. *Membranes 2022*, *12*(2), 160. https://doi.org/10.3390/membranes12020160

Martin, B., Okamura, S., Yasunaga, T., Ikegami, Y., & Ota, N. (2022). OTEC and advanced deep ocean water use for Kumejima: An introduction. *OCEANS 2022 - Chennai*, 1–5. https://doi.org/10.1109/OCEANSChennai45887.2022.9775240

Masutani, S. M., & Takahashi, P. K. (2001). Ocean thermal energy conversion (OTEC). *Encyclopedia of Ocean Sciences,* 1993–1999. https://doi.org/10.1006/rwos.2001.0031

Mencher, F. M., Spencer, R. B., Woessner, J. W., Katase, S. J., & Barclay, D. K. (2009). Growth of nori (Porphyra tenera) in an experimental OTEC-Aquaculture system in Hawaii. *Journal of the World Mariculture Society*, *14*(1–4), 458–470. https://doi.org/10.1111/j.1749-7345.1983.tb00098.x

Miller, A. & Ascari, M. (2011). *OTEC Advanced Composite Cold Water Pipe: Final Technical Report*. U.S. Department of Energy, Office of Scientific and Technical Information. https://doi.org/10.2172/1024183

Miller, A., Rosario, T., & Ascari, M. (2012). Selection and validation of a minimum-cost cold water pipe material, configuration, and fabrication method for ocean thermal energy conversion (OTEC) systems. In *Proceedings of SAMPE*. the Society for the Advancement of Material and Process Engineering. http://www.otecnews.org/wp-content/uploads/2012/07/Lockheed-Martin-OTEC-Cold-Water-pipe-SAMPE-2012-paper.pdf

Moriarty, P., & Wang, S. J. (2015). Assessing global renewable energy forecasts. *Energy Procedia*, *75*, 2523–2528. https://doi.org/10.1016/j.egypro.2015.07.256

Muralidharan, S. (2012). *Assessment of ocean thermal energy conversion* [Theses, Massachusetts Institute of Technology]. MIT Libraries. http://hdl.handle.net/1721.1/76927

Mutair, S., & Ikegami, Y. (2014). Design optimization of shore-based low temperature thermal desalination system utilizing the ocean thermal energy. *Journal of Solar Energy Engineering*, *136*(4), 041005. https://doi.org/10.1115/1.4027575

Naing, C., Reid, S. A., Aye, S. N., Htet, N. H., & Ambu, S. (2019). Risk factors for human leptospirosis following flooding: A meta-analysis of observational studies. *PloS One*, *14*(5), e0217643. https://doi.org/10.1371/journal.pone.0217643

Nakaoka, T., & Uehara, H. (1988). Performance test of a shell-and-plate type evaporator for OTEC. *Experimental Thermal and Fluid Science, 1(3)*, 283–291. https://doi.org/10.1016/0894-1777(88)90008-8

NOAA Office of Ocean & Coastal Resource Management. (2010). *Ocean thermal energy conversion (OTEC) environmental impacts* [Report]. National Oceanic and Atmospheric Administration. https://tethys.pnnl.gov/publications/ocean-thermal-energy-conversion-otecenvironmental-impacts

Nihous, G. C. (2007). A preliminary assessment of ocean thermal energy conversion resources. *Journal of Energy Resources Technology, 129*(1), 10–17. https://doi.org/10.1115/1.2424965

Nihous, G. C., & Vega, L. A. (1993). Design of a 100 MW OTEC-hydrogen plantship. *Marine Structures*, *6*(2–3), 207–221. https://doi.org/10.1016/0951-8339(93)90020-4

Novikov, I. I. (1958). The efficiency of atomic power stations (a review). In *Journal of Nuclear Energy (1954), 7*(1–2), 125–128. https://doi.org/10.1016/0891-3919(58)90244-4

Ocean Energy Systems. (2015). *International Levelised Cost of of Energy for Ocean Energy Technologies* [Report]. Ocean Energy Systems. https://tethys-engineering.pnnl.gov/sites/default/files/publications/oes.pdf

Ocean Energy Systems. (2018). An Overview of Ocean Energy Activities in 2018. *The Executive Committee of Ocean Energy Systems,* 146. https://tethys.pnnl.gov/sites/default/files/publications/oes2018_0.pdf

Panchal, C. B., & Bell, K. J. (1987). Simultaneous production of desalinated water and power using a Hybrid-Cycle OTEC plant. *Journal of Solar Energy Engineering*, *109*(2), 156–160. https://doi.org/10.1115/1.3268193

Petterson, M. G., & Kim, H. J. (2020). Can ocean thermal energy conversion and seawater utilisation assist small island developing states? A case study of Kiribati, Pacific Islands Region. In A. S. Kim & H.-J. Kim (Eds.), *Ocean Thermal Energy Conversion (OTEC), Past, present, progress.* IntechOpen. https://doi.org/10.5772/intechopen.91945

Prawira, Z., Koto, J., Sofyan Arief, D., Ilahude, D., Tasri, A., & Kamil, I. (2017). Cooling Pipe of Offshore Ocean Thermal Energy Conversion in Selat Makassar, Indonesia. In *International Journal of Environmental Research & Clean Energy, 5*(1), 7–16. https://isomase.org/IJERCE/Vol.10 Apr 2018/10-2.pdf

Rajagopalan, K., & Nihous, G. C. (2013). Estimates of global Ocean Thermal Energy Conversion (OTEC) resources using an ocean general circulation model. *Renewable Energy*, *50*, 532–540. https://doi.org/10.1016/j.renene.2012.07.014

Samsuri, N., Shaikh Salim, S. A. Z., Musa, M. N., & Mat Ali, M. S. (2016). Modelling performance of ocean-thermal energy conversion cycle according to different working fluids. *Jurnal Teknologi, 78*(11), 207–215. https://doi.org/10.11113/.v78.8741

Sasscer, D. S., & Ortabasi, U. (1979). Ocean thermal energy conversion (otec) tugboats for iceberg towing in tropical waters. In *Desalination* (Vol. 28).

Semmari, H., Stitou, D., & Mauran, S. (2012). A novel Carnot-based cycle for ocean thermal energy conversion. *Energy*, *43*(1), 361–375. https://doi.org/https://doi.org/10.1016/j.energy.2012.04.017

Setiawan, I. R., Purnama, I., & Halim, A. (2017). Increasing efficiency of a 33 MW OTEC in Indonesia using flat-plate solar collector for the seawater heater. *Journal of Mechatronics, Electrical Power, and Vehicular Technology*, *8*(1), 33–39. https://doi.org/10.14203/j.mev.2017.v8.33-39

Shukla, J. B., Verma, M., & Misra, A. K. (2017). Effect of global warming on sea level rise: A modeling study. *Ecological Complexity*, *32*(A), 99–110. https://doi.org/10.1016/j.ecocom.2017.10.007

Sinuhaji, A. R. (2015). Potential ocean thermal energy conversion (OTEC) in Bali. *KnE Energy*, *1*(1), 5–12. https://doi.org/10.18502/ken.v1i1.330

Spellman, F. R. (2016). *The science of renewable energy*. CRC Press.

Srinivasan, N. (2009). A new improved ocean thermal energy conversion system with suitable floating vessel design. In *Proceedings of the International Conference on Offshore Mechanics and Arctic Engineering - OMAE*, *4*(PART B) (1119–1129). The American Society of Mechanical Engineers. https://doi.org/10.1115/OMAE2009-80092

Sun, F., Ikegami, Y., Jia, B., & Arima, H. (2012). Optimization design and exergy analysis of organic rankine cycle in ocean thermal energy conversion. *Applied Ocean Research*, *35*, 38–46. https://doi.org/10.1016/j.apor.2011.12.006

Suparta, W. (2020). Marine heat as a renewable energy source. *Widyakala: Journal of Pembangunan Jaya University*, *7*(1), 37–41. https://doi.org/10.36262/widyakala.v7i1.278

Syamsuddin, M. L., Attamimi, A., Nugraha, A. P., Gibran, S., Afifah, A. Q., & Oriana, N. (2015). OTEC potential in the Indonesian seas. *Energy Procedia*, *65*, 215–222. https://doi.org/10.1016/j.egypro.2015.01.028

Tobal-Cupul, J. G., Garduño-Ruiz, E. P., Gorr-Pozzi, E., Olmedo-González, J., Martínez, E. D., Rosales, A., Navarro-Moreno, D. D., Benítez-Gallardo, J. E., García-Vega, F., Wang, M., Zamora-Castillo, S., Rodríguez-Cueto, Y., Rivera, G., García-Huante, A., Zertuche-González, J. A., Cerezo-Acevedo, E., & Silva, R. (2022). An assessment of the financial feasibility of an OTEC ecopark: A case study at Cozumel Island. *Sustainability. 14*(8), 4654. https://doi.org/10.3390/su14084654

Uehara, H., Dilao, C. O., & Nakaoka, T. (1988). Conceptual design of ocean thermal energy conversion (OTEC) power plants in the Philippines. *Solar Energy, 41*(5), 431–441. https://doi.org/10.1016/0038-092X(88)90017-5

Uehara, H., Ikegami, Y., & Nishida, T. (1998). Performance analysis of OTEC system using a cycle with absorption and extraction processes. *Transactions of the Japan Society of Mechanical Engineers Series B*, *64(624),* 2750–2755. https://doi.org/10.1299/kikaib.64.2750

Uehara, H., Miyara, A., Ikegami, Y., & Nakaoka, T. (1996). Performance analysis of an OTEC plant and a desalination plant using an integrated hybrid cycle. *Journal of Solar Energy Engineering, 118*(2), 115–122. https://doi.org/10.1115/1.2847976

Vega, L. A. (2002). Ocean thermal energy conversion primer. *Marine Technology Society Journal, 36*(4): 25–35. https://doi.org/10.4031/002533202787908626

Vega, L. A. (2013). Ocean thermal energy conversion. In M. Kaltschmitt, N. J. Themelis, L. Y. Bronicki, L. Soder, & L. A. Vega (Eds.). *Renewable energy systems* (1273–1305). Springer. https://doi.org/10.1007/978-1-4614-5820-3_695

Wang, C. M., & Wang, B. T. (2015). Great ideas float to the top. *Large Floating Structures*, *3*, 1–36. https://doi.org/10.1007/978-981-287-137-4_1

Wang, C. M., Yee, A. A., Krock, H., & Tay, Z. Y. (2011). Research and developments on ocean thermal energy conversion. *IES Journal Part A: Civil and Structural Engineering*, *4*(1), 41–52. https://doi.org/10.1080/19373260.2011.543606

Wang, T., Ding, L., Gu, C., & Yang, B. (2008). Performance analysis and improvement for CC-OTEC system. *Journal of Mechanical Science and Technology*, *22*(10), 1977–1983. https://doi.org/10.1007/s12206-008-0742-9

Welsh, K., & Bowleg, J. (2022). Interventions and solutions for water supply on small islands: The case of New Providence, The Bahamas. *Frontiers in Water*, 4. https://doi.org/10.3389/frwa.2022.983167

Wu, C. (1987). A performance bound for real OTEC heat engines. *Ocean Engineering, 14*(4): 349–354. https://doi.org/10.1016/0029-8018(87)90032-1.

Xiang, S., Cao, P., Erwin, R., & Kibbee, S. (2013). OTEC cold water pipe global dynamic design for ship-shaped vessels. In *Proceedings of the ASME 2013 32nd International Conference on Ocean, Offshore and Arctic Engineering, Volume 8: Ocean Renewable Energy:* Paper V008T09A060. American Society of Mechanical Engineers. https://doi.org/10.1115/OMAE2013-10927

Yang, M. H., & Yeh, R. H. (2014). Analysis of optimization in an OTEC plant using organic Rankine cycle. *Renewable Energy*, *68*, 25–34. https://doi.org/10.1016/j.renene.2014.01.029

Yasunaga, T., Fontaine, K., & Ikegami, Y. (2021). Performance evaluation concept for ocean thermal energy conversion toward standardization and intelligent design. *Energies*, *14*(8), 2336. https://doi.org/10.3390/en14082336

Yasunaga, T., & Ikegami, Y. (2020). Finite-time thermodynamic model for evaluating heat engines in ocean thermal energy conversion. *Entropy*, *22*(2), 211. https://doi.org/10.3390/e22020211

Yoshizuka, K., Holba, M., Yasunaga, T., & Ikegami, Y. (2007). Performance evaluation of benchmark plant for selective lithium recovery from seawater. *Journal of Ion Exchange, 18*(4), 450–453. https://doi.org/10.5182/jaie.18.450

Yoshizuka, K., Holba, M., Yasunaga, T., & Ikegami, Y. (2007). Performance evaluation of benchmark plant for selective lithium recovery from seawater. *Journal of Ion Exchange, 18*(4), 450–453. https://doi.org/10.5182/jaie.18.450

Zulqarnain, Mohd Yusoff, M. H., Keong, L. K., Yasin, N. H., Rafeen, M. S., Hassan, A., Srinivasan, G., Yusup, S., Shariff, A. M., & Jaafar, A. B. (2023). Recent development of integrating CO2 hydrogenation into methanol with ocean thermal energy conversion (OTEC) as potential source of green energy. *Green Chemistry Letters and Reviews, 16*(1), 2152740.. Taylor and Francis Ltd. https://doi.org/10.1080/17518253.2022.2152740